

2. SITE 544¹

Shipboard Scientific Party^{2, 3}

HOLE 544

Date occupied: 17 April 1981
Date departed: 19 April 1981
Time on hole: 1 day, 17 hr., 41 min.
Position: 33°46.0'N; 09°24.3'W
Water depth (sea level; corrected m, echo-sounding): 3607
Water depth (rig floor; corrected m, echo-sounding): 3617
Bottom felt (m, drill pipe): 3675 (beneath rig floor)
Penetration (m): 5
Number of cores: 1
Total length of cored section (m): 5
Total core recovered (m): 5.6
Core recovery (%): 112
Oldest sediment cored:
Depth sub-bottom (m): 3681
Nature: Pelagic nannofossil ooze
Age: late Pleistocene
Basement: Not reached

HOLE 544A

Date occupied: 19 April 1981
Date departed: 21 April 1981
Time on hole: 2 days, 6 hr., 57 min.

Position: 33°46.0'N; 09°24.3'N
Water depth (sea level; corrected m, echo-sounding): 3581
Water depth (rig floor; corrected m, echo-sounding): 3591
Bottom felt (m, drill pipe): 3617 (beneath rig floor)
Penetration (m): 235
Number of cores: 28
Total length of cored section (m): 235
Total core recovered (m): 83.1
Core recovery (%): 35.5
Oldest sediment cored:
Depth sub-bottom (m): 139.3
Nature: Grayish red sandy mud
Age: late Triassic-Early Jurassic
Measured velocity (km/s): 1.67–1.8
Basement:
Depth sub-bottom (m): 184.4
Nature: Granitic gneiss
Velocity range (km/s): 5.7

HOLE 544B

Date occupied: 21 April 1981
Date departed: 23 April 1981
Time on hole: 1 day, 6 hr., 15 min.
Position: 33°46.0'N; 09°24.3'W
Water depth (sea level; corrected m, echo-sounding): 3581
Water depth (rig floor; corrected m, echo-sounding): 3591
Bottom felt (m, drill pipe): 3617 (beneath rig floor)
Penetration (m): 39.3
Number of cores: 12
Total length of cored section (m): 39.3
Total core recovered (m): 37.0
Core recovery (%): 94
Oldest sediment cored:
Depth sub-bottom (m): 39.3
Nature: Pelagic foraminiferal-nannofossil ooze
Age: late Miocene
Measured velocity (km/s): 1.5
Basement: Not reached

Principal results: At Site 544, on a structural high block in front of the Mazagan Plateau (Fig. 1), drilling established the presence of gneissic basement beneath Upper Jurassic limestone and red sandy mudstone that is earlier than the Late Jurassic (Fig. 2).

1. In Hole 544 (250 m northwest of Hole 544A), Pleistocene foraminiferal-nannofossil ooze was cored in a single core 0–5 m beneath the seafloor (BSF).

2. In Hole 544A, the section drilled (Fig. 2) consisted of five units.

Unit I: 0–102 m BSF, yellow-brown foraminiferal nannofossil ooze of Pleistocene to early middle Miocene age (Zone N9). This unit includes a hiatus spanning the late middle Miocene to early late Miocene (Zones N14–N17).

¹ Hinz, K., Winterer, E. L., et al., *Init. Repts. DSDP*, 79: Washington (U.S. Govt. Printing Office).

² Karl Hinz (Co-Chief Scientist), Bundesanstalt für Geowissenschaften und Rohstoffe, 3 Hannover, Postfach 510153, Federal Republic of Germany; E. L. Winterer (Co-Chief Scientist), Geological Research Division, Scripps Institution of Oceanography, La Jolla, CA 92093; Peter O. Baumgartner, Geological Research Division, Scripps Institution of Oceanography, La Jolla, CA 92093 (present address: Escuela Centroamericana de Geología, Apartado 35, Ciudad Universitaria Rodrigo Facio, San José, Costa Rica); Martin J. Bradshaw, Department of Geological Sciences, University of Aston, Birmingham B4 7ET, United Kingdom (present address: Shell International Petroleum Company, The Hague, The Netherlands); James E. T. Channell, Lamont-Doherty Geological Observatory, Columbia University, Palisades, New York (present address: Department of Geology, 1112 GPA Building, University of Florida, Gainesville, Florida 39611); Michel Jaffrezou, Département de Géotectonique, Université Pierre et Marie Curie, 4 place Jussieu, 75230 Paris Cedex 05, France; Lubomir F. Jansa, Geological Survey of Canada, Bedford Institute of Oceanography, Dartmouth, Nova Scotia, Canada; Robert Mark Leckie, Department of Geological Sciences, University of Colorado, Boulder, Colorado 80309 (present address: Department of Geology and Geography, University of Massachusetts, Amherst, Massachusetts 01003); Johnnie N. Moore, Department of Geology, University of Montana, Missoula, Montana 59812; Jürgen Rullkötter, Institut für Erdöl und Organische Geochemie, ICH-5, KFA Jülich, Postfach 1913, D-517 Jülich, Federal Republic of Germany; Carl H. Schaftenaar, Department of Geophysics, Texas A&M University, College Station, Texas 77843 (present address: Chevron, U.S.A., 700 S. Colorado Blvd., Denver, Colorado 80222); Torsten H. Steiger, Institut für Paläontologie und Historische Geologie, Universität München, Richard-Wagner-Strasse 10, D-800 München 2, Federal Republic of Germany; Vassil T. Vuchev, Kansas Geological Survey, University of Kansas, Lawrence, Kansas 66044 (present address: Geological Institute, Bulgarian Academy of Sciences, UL. Academy G. Bonchev, Block 2, 1113 Sofia, Bulgaria); and George E. Wiegand, Department of Geology, Florida State University, Tallahassee, Florida 32306.

³ The descriptions of sites, cores, and data included in these site reports were completed within one year of the cruise, but many of the topical chapters that follow were completed at a later date. More data were acquired and authors' interpretations matured during this interval, so readers may find some discrepancies between site reports and topical papers. This is particularly true of biostratigraphic age assignments. The timely publication of the *Initial Reports* series, which is intended to report the early results of each leg, precludes incurring the delays that would allow the site reports to be revised at a later stage of production.

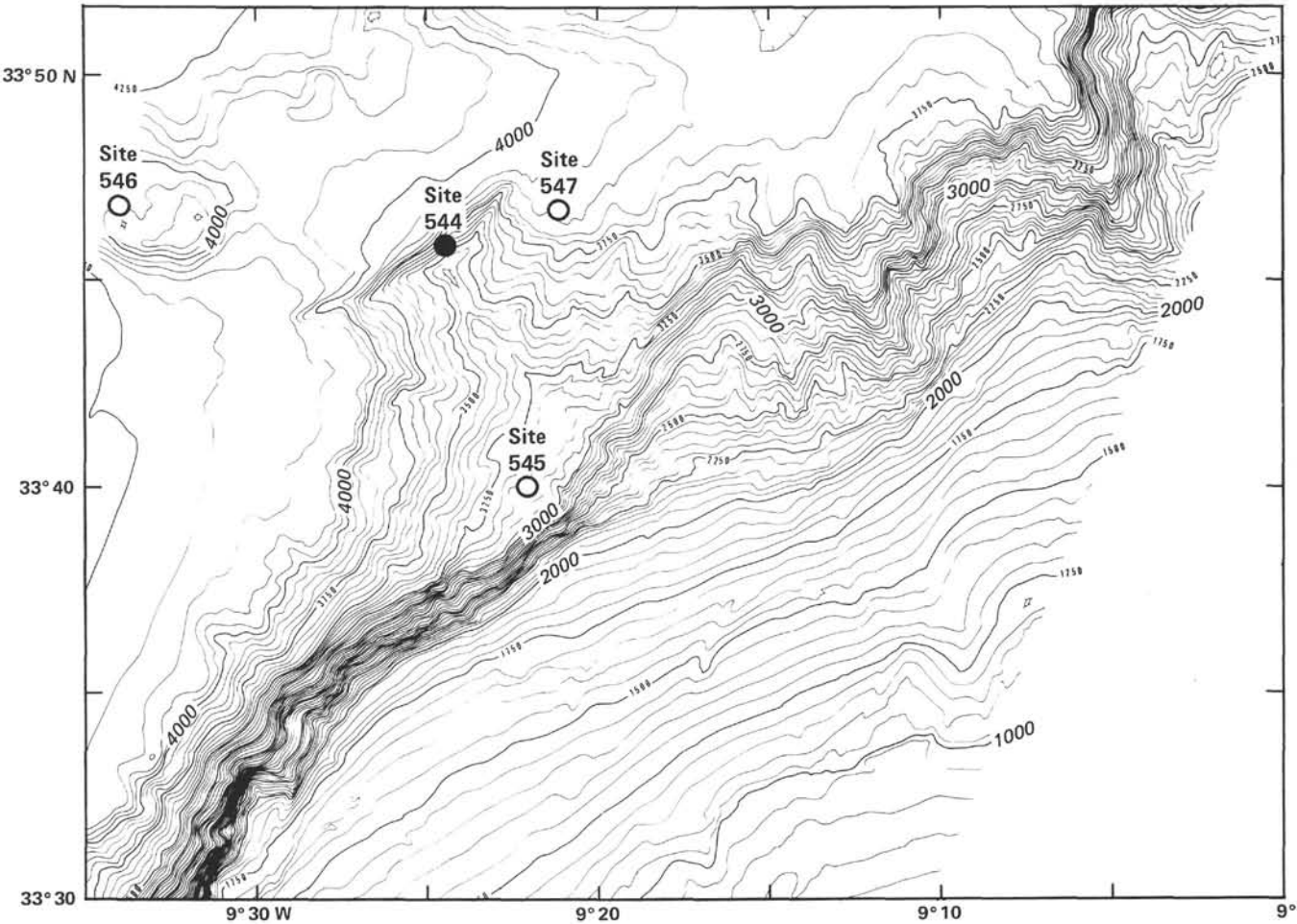


Figure 1. Bathymetry around Site 544, based on SEAZAGAN Seabeam map (Auzende et al., this volume). Depths in m.

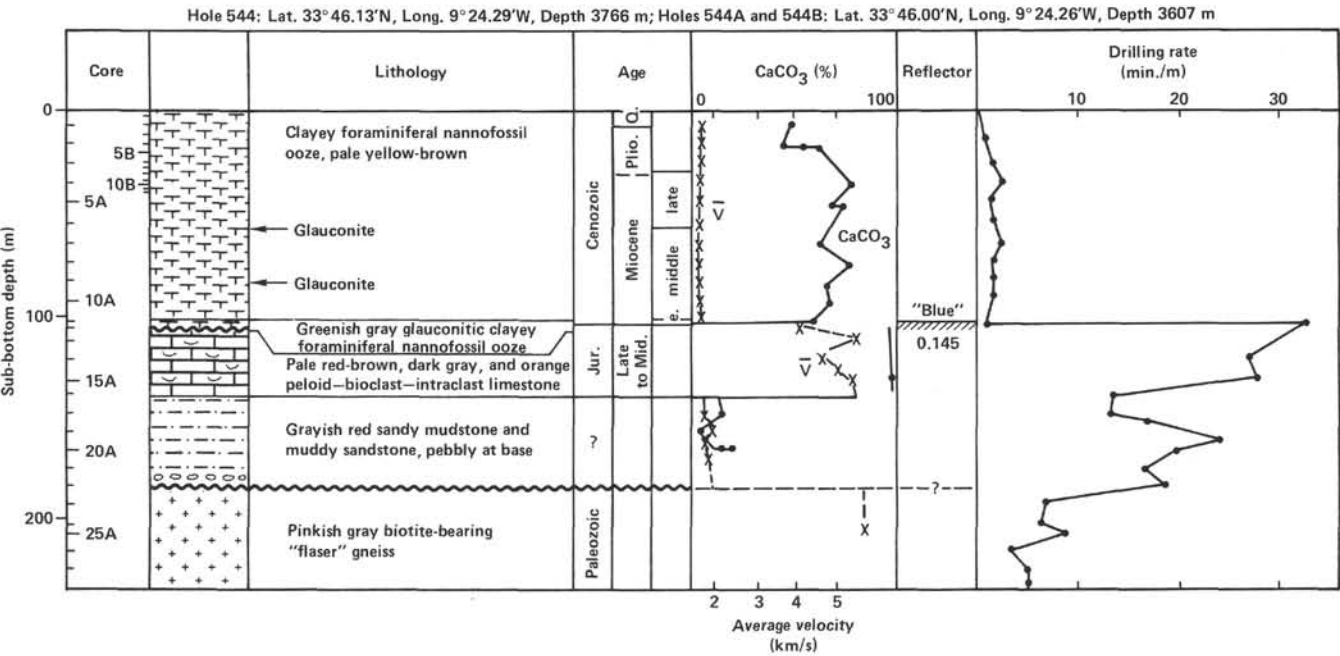


Figure 2. Summary graphic log of Site 544 (chiefly Hole 544A). A and B indicate cores from Holes 544A and 544B, respectively.

Unit II: 102–103.8 m BSF, greenish gray clayey nannofossil-foraminiferal ooze, with glauconite and Fe–Mn crusts and micronodules, of early Miocene age (Zone N7).

Unit III: 103.8–139.2 m BSF, pale red-brown mottled limestone. Coated-intraclast packstone with subordinate grainstone and wackestone. Abundant cyanobacterial coatings on bioclasts. Contains *Protoglobigerina*, thin-shelled pelagic mollusks, and ammonites, plus a rich benthic fauna including *Pentacrinus*, ostracodes, small gastropods, miliolids, sponge fragments, serpulids, and bryozoans. Includes hardgrounds with borings and encrusting fauna. Closely resembles Oxfordian limestone dredged from Mazagan Escarpment. Outer neritic facies.

Unit IV: 139.2–184.3 m BSF, reddish brown calcareous and sandy mudstone and muddy sandstone, with gneissic pebbles near the base. Includes mud flows near the top. Continental facies.

Unit V: 184.3–235 m BSF (T.D.), granitic gneiss with cataclastic flaser textures. Subhorizontal foliation.

3. In Hole 544B (same location and depth as 544A), a section from 0–39 m (T.D.) was hydraulic piston cored; recovered were lower Pleistocene to upper Miocene sediments with abundant and well-preserved foraminifers and nannofossils, but no radiolarians.

BACKGROUND AND OBJECTIVES

Seaward of the Mazagan Escarpment and slope is a band about 50 km wide where structures interpreted as diapirs stand like columns within a pile of sediments about 5 km thick (Fig. 1). Dredges and cores from *Vema* cruise 30-13 and *Valdivia* cruise West Africa 1979 on the slopes of the most landward of these structural highs, just 10 km from the foot of the escarpment (Figs. 3 and 4), recovered fragments of sheared granite. We believed that, if this structure were a salt diapir, it might have carried upward very old sediments, dating to the earliest stages of Atlantic evolution, in the Early Jurassic or late

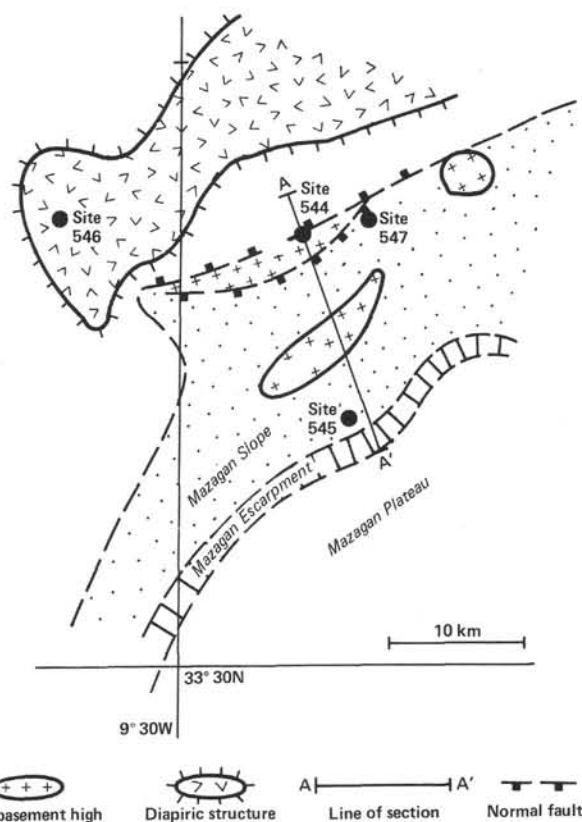


Figure 4. Map of Mazagan Escarpment area, showing Leg 79 sites and major geologic features. Line A-A' is line of seismic reflection profile M 53-08.

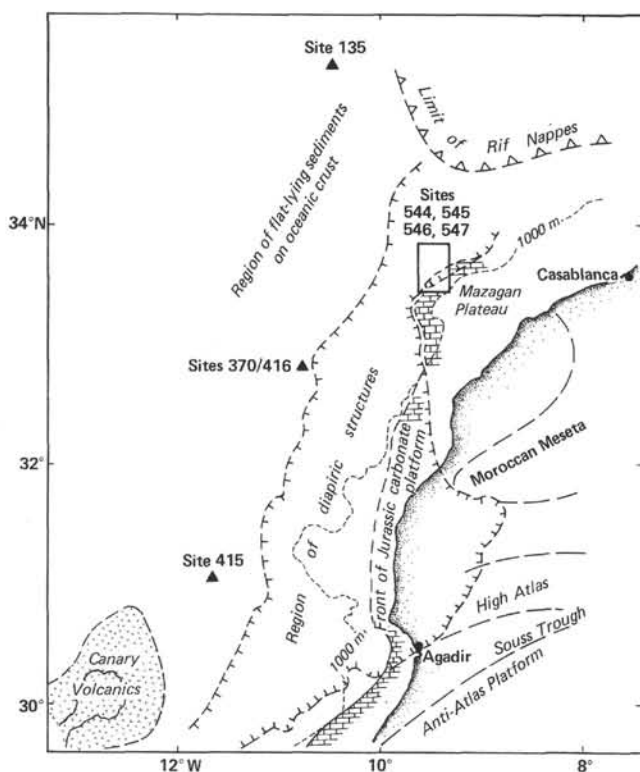


Figure 3. Map showing the regional setting of the Mazagan Plateau. The area inside the square is shown in greater detail in Figure 4.

Triassic. Alternatively, the dredged fragments of granite suggested that this particular structure might be a Hercynian basement high rather than a salt diapir, and this case we might also be able to obtain samples of the earliest sediments deposited on basement. Drilling on this particular structure was approved by the JOIDES Safety and Pollution Prevention Panel, provided sites were located so as to avoid the possibility of encountering hydrocarbons.

Two sites were planned on this structure: one down the north flank of the structure where the sedimentary section is fairly thick (Site MAZ-9 during the planning stage; actually drilled as Site 547); and another located high on the structure and along its northeast flank, where Mesozoic rocks may have cropped out prior to Cenozoic times, and close to the localities where the granite fragments occur on the seafloor. This latter site (Site MAZ-3 during the planning stage) we chose to drill as Site 544, the first site occupied on Leg 79.

Objectives at Site 544 (MAZ-3)

The prime objective at Site 544 was to determine the nature of the deepest layers seen on the seismic profiler records (e.g., profile M53-08, Figs. 4 and 20): is it "granite" or is it salt? The strategy for the site was to drill on the seaward flank of the seismic structure, near where the deepest strong reflector actually crops out, and where the risk of encountering any hydrocarbon accumulation is minimal. At planning Site MAZ-3 (and nearby MAZ-

2) there is just enough (about 100 m) of what we interpreted as soft Cenozoic hemipelagic sediments to bury the bottom-hole assembly before drilling encounters the strong reflector, which we believed might be hard rock and might require considerable weight on the bit and rotation of the drill string to penetrate. By close monitoring of cores for the salinity of interstitial waters and for the presence of hydrocarbons, we could expect timely warning of the possible presence of a salt diapir below or of the danger of hydrocarbon accumulation.

If the "basement" were salt, we hoped to learn something of the history of vertical movements by halokinesis from the stratigraphy of the overlying beds. If the basement were granitic, we hoped to learn something of the early history of subsidence and drowning of what would appear to be close to the seawardmost edge of the African continent as it broke away from North America.

We also planned to collect hydraulic piston cores of the Cenozoic section for a detailed picture of the evolution of hemipelagic environments in response to both local vertical tectonics and to more regional paleoceanographic events.

OPERATIONS

Leg 79 began on 15 April 1981, when *Glomar Challenger* steamed out of Las Palmas toward the Mazagan Plateau. The approach to the first site, chosen to be as close to planning Site MAZ-3 as possible, was made by trying to follow along the *Meteor* 53-08 multichannel seismic line (Fig. 5). But as luck would have it, about 2 hr. before we were scheduled to turn onto that line, the ship's satellite navigation system failed, and we had to navigate as best we could, using both the detailed bathymetric chart prepared from all existing precision-navigated soundings in the area and the subsurface data from the *Meteor* seismic lines. The ship's Omega navigation system proved quite unreliable at the resolution we required.

Nonetheless, with only minor course corrections we passed very close to MAZ-3, which was recognizable from a very distinctive small valley-and-hill sequence, as well as from the geometry of subsurface reflectors (Fig. 5). After steaming about one mile beyond the chosen site, the ship made a Williamson turn and returned to the site, where the drill crew released a 13.5 kHz acoustic beacon, at 1952 hr. on 17 April. A chart of the approach is shown in Figure 5.

Water depth at the beacon was measured from the echo sounder as 3586 uncorrected m. When corrected for the velocity of sound in this region (area 13; Matthews, 1939) and for the depth of the hydrophones on the ship's hull, the depth of Site 544 was temporarily established as 3607 m below sea level (3617 m below the derrick floor), pending more information from the drill itself.

Because Site 544 is on a steep slope (probably more than 15°), the wide-angle echo sounder does not give a true picture of the profile of the seafloor, but rather draws a series of hyperbolae representing echoes from sharp changes in slope. We were thus virtually certain

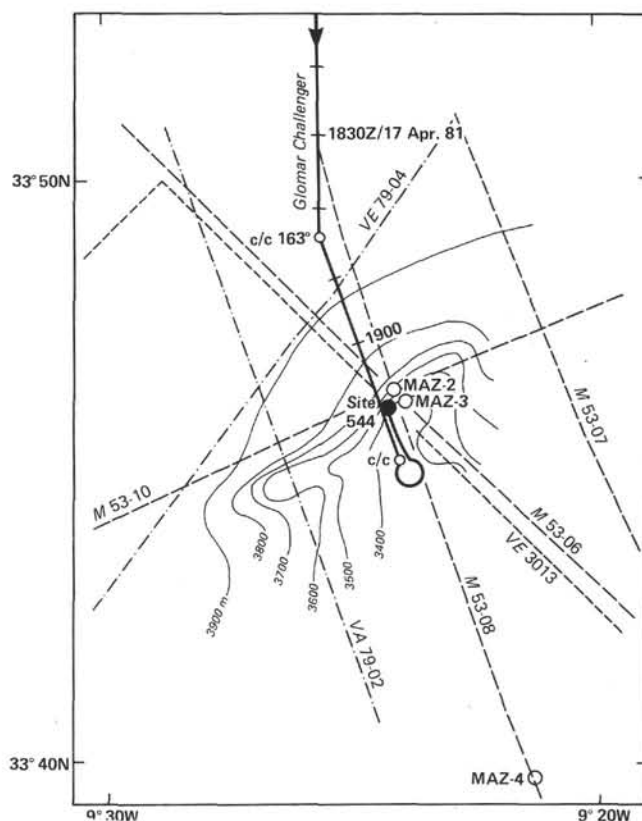


Figure 5. Approach to Site 544.

that the seafloor lay below the trace seen on the echo sounder record. But to be on the safe side, the drill string was lowered so as to place the bit about 2.5 m above the 3617-m "nominal" depth and then lowered slowly to 3617 m. The first coring attempt was from 3617 to 3624 m, and the core barrel returned empty, as expected. We continued in this fashion, 9.5 m at a time, until the weight indicator showed the bit had arrived on the seafloor. The core taken in the interval 3671.5 to 3681 m contained 5 m of highly disturbed sediment, and we therefore established the actual depth of the seafloor at Hole 544 as 3675 m below the derrick floor (3665 m below sea level), or some 58 m below the echo sounder trace.

Close inspection of the seismic profiler record at Hole 544 showed us that if the near-surface sediments were stiff we might have difficulty burying the drill collars to a depth sufficient to allow drilling in hard rocks, so we decided to discontinue drilling at this hole and move the ship 250 m to the southeast, on course 163°, which would bring us a little farther upslope to a point where we could spud in slightly younger sediments and have an adequate thickness of soft sediments above the first prominent reflector on the seismic profile. Hole 544 was abandoned at 1333 hr. on 19 April 1981.

Hole 544A

After the move from Hole 544, the new depth was estimated from the echo sounder as 3560 uncorrected meters, or 3591 corrected meters below the derrick floor.

The pipe, which had been raised about 100 m above the seafloor during the move, was lowered slowly, searching for the seafloor. In the interval 3605–3624 m, we touched bottom at 1614 hr. on 18 April, and Core 544A-1 was retrieved with 6.8 m of ooze within. On this basis the seafloor depth for Hole 544A was established at 3617 m below the derrick floor.

Coring proceeded 9.5 m at a time through Neogene calcareous ooze, which by core 544A-2 was already stiff enough to require rotation of the bit, and by Core 544A-8, at a sub-bottom depth of 64 m, to require slow circulation. Gradually increasing pump pressure and speed of rotation were required as the coring proceeded, until the upper part of the interval 3719–3724.5 m, where the drill met a very resistant layer. This core (544A-12) contained a small piece of hard, reddish limestone in the core catcher and marked the top of a sequence of similar hard limestone beds some 25 m thick, which cored very slowly (about 30 min./m). Recovery rates in this limestone were fair (about 50%), but in the next underlying unit, consisting mainly of red mudstone, the recovery rate was rather poor (about 20%). At about 3801 m, at the beginning of Core 544A-23, the drilling rate speeded up to about 7 min./m, and this rate was maintained or even increased slightly all the way through the last core (544A-28), even though we were coring in gneissic basement rocks.

After Core 544A-28 was retrieved at 1035 hr. on 25 April, a barrel was dropped to the bottom again, but the pipe became stuck in the hole and the Cruise Operations Manager advised abandoning the hole. The pipe was freed after several attempts, but the overshot sent to pick up the core barrel could not retrieve it, even after several attempts, and the drill string was pulled with the barrel in place, arriving back on deck at 2030 hr. on 21 April 1981. An examination of it showed that disintegration of a steel ring in the hydraulic bit-release mechanism above the bit had prevented the mechanism from operating.

Hole 544B

Hole 544B is at the same location as Hole 544A; drilling there represented an attempt to obtain a continuous sequence of hydraulic piston cores through the Neogene sediment at this site.

The crew began to run pipe at 2030 hr. on 21 April 1981 and Core 544B-1 was spudded at 0505 hr. on 22 April. From the very first core, the recovery was less than the 4.4-m length of stroke of the hydraulic piston corer (HPC), because of the firmness of the sediments. After 12 cores, the bit had advanced only 39.3 m, and the recovery was less than 2 m in Core 544B-12. We thus decided to terminate operations, since we had passed the Miocene/Pliocene biostratigraphic boundary (probably in Core 544B-10 or 544B-11), and one of the principal objectives, which was to core sediments coeval with the end of the Messinian salinity "crisis" of the Mediterranean, had been reached.

Disturbance of the cores was minimal except in two cores in which the plastic core liner cracked or broke away under the impact of the coring process; these contained some severely deformed intervals.

The measured vane shear strength of the HPC cores from Hole 544B was uniformly about twice as high as cores from equivalent depths in Hole 544A, showing what changes in mass properties are effected by conventional coring methods. But the highest shear strength measured, on the deepest HPC cores, was less than 100 kPa (1 kg/cm²), a value somewhat less than we had assumed would limit HPC operations.

The drill string was retrieved and the ship was underway for Site 545 at 0245 hr. on 23 April 1981.

A summary of the coring operations, giving core numbers and depths, is shown in Table 1.

SEDIMENT LITHOLOGY

At Site 544, three holes (544, 544A, and 544B) were drilled on the northwestern flank of the escarpment in depths from derrick floor of 3675 m (544) and 3617 m (544A and 544B). The drilled section is shown in summary form in Figure 2, and in greater detail in Figure 23.

Hole 544

In Hole 544, 5 m of disturbed core were recovered, consisting entirely of clayey foraminiferal-nannofossil ooze (Unit I) of early middle Pleistocene age.

Table 1. Coring summary, Site 544.

Core no.	Date (April 1981)	Time	Depth from drill floor (m)		Depth below seafloor (m)		Length cored (m)	Length recovered (m)	Percentage recovered
			Top	Bottom	Top	Bottom			
Hole 544									
1	18	1333	3676.0	3681.0	0.0	5.0	5.0	5.0	100
Hole 544A									
1	18	1655	3617.0	3624.0	0.0	7.0	7.0	6.8	97
2	18	1805	3624.0	3633.5	7.0	16.5	9.5	9.0	95
3	18	1927	3633.5	3643.0	16.5	26.0	9.5	3.8	40
4	18	2058	3643.0	3652.5	26.0	35.5	9.5	3.1	33
5	18	2217	3652.5	3662.0	35.5	45.0	9.5	3.5	37
6	18	2343	3662.0	3671.5	45.0	54.5	9.5	5.7	60
7	19	0114	3671.5	3681.0	54.5	64.0	9.5	4.6	48
8	19	0237	3681.0	3690.5	64.0	73.5	9.5	5.4	57
9	19	0405	3690.5	3700.0	73.5	83.0	9.5	5.3	56
10	19	0538	3700.0	3709.5	83.0	92.5	9.5	8.1	85
11	19	0701	3709.5	3719.0	92.5	102.0	9.5	0.8	8
12	19	0901	3719.0	3724.5	102.0	107.5	5.5	1.8	33
13	19	1216	3724.5	3728.5	107.5	111.5	4.0	2.0	50
14	19	1752	3728.5	3738.0	111.5	121.0	9.5	5.0	53
15	19	2312	3738.0	3747.0	121.0	130.0	9.0	5.4	60
16	20	0227	3747.0	3756.0	130.0	139.0	9.0	1.2	13
17	20	0540	3756.0	3765.0	139.0	148.0	9.0	0.3	3
18	20	0717	3765.0	3766.5	148.0	149.5	1.5	0.1	7
19	20	1113	3766.5	3774.0	149.5	157.0	7.5	0.8	11
20	20	1514	3774.0	3783.0	157.0	166.0	9.0	4.6	51
21	20	1858	3783.0	3792.0	166.0	175.0	9.0	2.1	23
22	20	2248	3792.0	3801.0	175.0	184.0	9.0	1.0	11
23	21	0055	3801.0	3810.0	184.0	193.0	9.0	0.3	3
24	21	0258	3810.0	3819.0	193.0	202.0	9.0	0.6	7
25	21	0600	3819.0	3823.5	202.0	206.5	4.5	0.4	9
26	21	0742	3823.5	3833.0	206.5	216.0	9.5	0.5	5
27	21	0931	3833.0	3842.5	216.0	225.5	9.5	0.4	4
28	21	1127	3842.5	3852.0	225.5	235.0	9.5	0.5	5
							235.0	83.1	35
Hole 544B									
1	22	0705	3617.0	3619.4	0.0	2.4	2.4	3.2	133
2	22	0811	3619.4	3623.8	2.4	6.8	4.4	4.3	98
3	22	0912	3623.8	3628.2	6.8	11.2	4.4	3.9	89
4	22	1016	3628.2	3632.6	11.2	15.6	4.4	3.1	70
5	22	1119	3632.6	3637.0	15.6	20.0	4.4	3.9	89
6	22	1221	3637.0	3641.4	20.0	24.4	4.4	3.7	84
7	22	1333	3641.4	3644.4	24.4	27.4	3.0	3.2	107
8	22	1427	3644.4	3647.9	27.4	30.9	3.5	3.5	100
9	22	1539	3647.9	3650.7	30.9	33.7	2.8	2.8	100
10	22	1734	3650.7	3653.4	33.7	36.4	2.7	2.6	96
11	22	1838	3653.4	3654.4	36.4	37.4	1.0	0.9	90
12	22	1935	3654.4	3656.3	37.4	39.3	1.9	1.9	100
							39.3	37.0	94

Unit I (0–5 m; Core 1)

Unit I consists of 5 m of predominantly light brown (5YR 6/4) clayey foraminiferal nannofossil ooze; carbonate bomb analysis indicates about 51% CaCO_3 . Pale, grayish orange-pink (5YR 7/2) interlayers are common below 2 m and contain a higher proportion of foraminifer tests. The basal 75 cm of the core becomes more gray, assuming a pale yellowish brown color (10YR 6/2). Additional biogenic components include rare fish remains. A small terrigenous silt to very fine sand fraction consists largely of quartz grains with trace amounts of feldspar, heavy minerals, mica, amphiboles, and pyroxenes. Silt-sized dolomite rhombs compose 1–2% of the sediment. Darker colored, highly deformed burrow traces were observed at several levels.

Discussion: This unit is clearly a pelagic sediment, deposited above the carbonate lysocline with an input of terrigenous clay and siliciclastic material from the shelf (?coast). A lamina of foraminiferal sand suggests an increase of bottom current activity which produced sediment reworking.

A similar lithologic unit was encountered during Leg 50 in Core 415-1, located on the northern flank of Agadir Canyon, about 150 km from the Moroccan coast. Sediments of an equivalent age at Site 370 (Leg 41), located in the deeper part of the Moroccan Basin, are similar but contain more terrigenous detritus; their greenish gray color indicates a thinner layer of oxygenated surface sediment.

Hole 544A

Hole 544A was penetrated to a depth of 235 m below the seafloor. Total core recovery was 35%.

Five main lithological units are recognized. Unit I, a pale yellowish brown clayey foraminiferal nannofossil ooze (102 m), and Unit II, greenish gray and greenish yellow biogenic calcareous oozes and clays (1.8 m), constitute the Cenozoic sequence (lower Pleistocene to lower Miocene). These rest unconformably on 35.4 m of ?Middle to ?Upper Jurassic reddish-colored peloid-skeletal-intraclastic limestones, which make up Unit III. Unit IV consists of 45.1 m of grayish red sandy muds with pebbly muddy sands and muddy gravels at their base, overlying a gneissic basement (Unit V), into which the bit penetrated 50.7 m. The lithologic units are described below in detail, in descending order.

Unit I: 0 to 102.0 m; Cores 544A-1 to 544A-11

Unit I, 102 m thick, is dominantly pale yellowish brown (10YR 6/2), clayey (illitic) foraminiferal nannofossil ooze of early Pleistocene to early middle Miocene age. Terrigenous quartz content is variable but low throughout.

A color change from pale yellowish brown to grayish orange pink (5YR 7/2) below Core 544A-3 is accompanied by a steady drop in foraminifer content. Carbonate content increases downward, rising from 50 to 79% in Core 8, then falling to 60% near the base of the unit (Table 2). Cores 544A-7 and 544A-8 differ from the others in their olive gray colors (5Y 6/1, N7, 5YR 4/1, 5YR

Table 2. Carbonate Bomb analyses, Hole 544A.

Core-Section (interval in cm)	Lithology	CaCO ₃ (%)
Unit I		
1-1, 142-144	Clayey foraminifer-nannofossil ooze	49.5
1-1, 144-150		53.0
1-2, 90-92		57.4
1-4, 100-102		64.2
2-4, 142-144	Clayey nannofossil-foraminifer ooze	41.5
2-4, 144-150		54.5
2-5, 118-120		57.0
2-6, 0-2		62.0
3-6, 105-106	Slightly clayey foraminifer-nanno- fossil ooze	56.9
4-1, 144-150		69.1
4-2, 73-79		78.8
5-2, 28-29		69.4
5-2, 118-120	Slightly clayey nannofossil ooze	72.6
5-3, 0-2		69.6
6-4, 40-41		75.2
7-1, 130-132		61.0
7-2, 10-12	Clayey nannofossil ooze	67.3
8-2, 20-22	Clayey foraminifer-nannofossil ooze	79.9
8-2, 144-150	Slightly clayey nannofossil ooze	77.1
8-3, 118-120		76.1
8-4, 0-2	Slightly clayey nannofossil-foramini- fer ooze	71.6
9-1, 65-66	Clayey foraminifer-nannofossil ooze	70.5
9-1, 70-72		65.0
10-2, 80-82	Clayey nannofossil ooze	66.0
10-2, 85-86		60.0
Unit II		
12-1, 37-39	Clayey nannofossil-foraminifer ooze	58.5
12-1, 39-40		74.1
12-2, 11-13	Nannofossil-bearing clay	3.1
Unit III		
15-3, 120-104	Oncoïd-peloid-bioclast-intraclast packstone	100.0
Unit IV		
17-1, 26-27	Dark red-brown sandy mud	11.5
19-1, 79-81	Dark red-brown muddy sand	3.7
20-2, 118-120	Grayish red sandy mud	18.3
20-3, 0-2	Grayish red/gray-olive muddy sand	14.1
20-3, 5-6		16.7

6/5, and 5Y 5/2); this interval is a slightly clayey nannofossil ooze of late Miocene to middle Miocene age, containing common glauconite and pyrite framboids. The downward change occurs by interlayering within Section 544A-7-1, between 45 and 84 cm. The reappearance of significant quantities of foraminifers in Core 544A-8 is followed by a return to pale yellowish brown colors in Core 544A-9.

Though drilling disturbance (severe in the upper half of Unit I) creates problems in confidently elucidating sedimentary structures, we observed throughout 2–5 mm interlayering, generally consisting of slightly darker and paler shades of the principal sediment color. Also occurring throughout Unit I, though sporadically, are dark gray to black millimeter-thick layers, rich in iron sulfide; burrow fills of a similar material are generally expressed by tiny dark gray to black patches or spots, about 4 mm in diameter.

Discussion: Unit I consists of pelagic sediment deposited above the foraminiferal lysocline, with a terrigenous input varying between 20 and 50%, represented mostly by clay.

The pale yellowish brown and grayish orange pink colors reflect a thick surface layer of oxygenated sediment during deposition; this layer may have been thinner during formation of the grayer, more pyritic interval in Cores 544A-7 and 544A-8. Stratigraphic condensation within the latter is expressed sedimentologically by common glauconite. We suggest that the iron sulfide layers and burrow fills formed in reducing microenvironments owing to locally high concentrations of organic matter. The lower boundary of Unit I is placed at the base of Core 11 at the color change from pale yellowish brown to light greenish gray.

Unit II: 102.0–103.8 m; Core 544A-11

Unit II is 1.8 m thick, of lower Miocene age, and is contained entirely within Core 12. A prominent, 4-cm thick, dusky green (5G 3/2) layer below 60 cm in Section 1 consists of clayey foraminiferal nannofossil ooze containing lithified clayey foraminiferal wackestone. Dusky red (10R 2/2) mottling is the result of patchy oxidation of this essentially Fe–Mn crust, which marks a hiatus embracing the upper lower Miocene (foraminiferal biostratigraphic data). Below this layer, dusky yellow green (5GY 5/2) and grayish olive green (5GY 3/2) glauconite-rich calcareous claystone grades down, through yellowish gray (5Y 8/1), slightly clayey, calcareous ooze (resulting probably from the recrystallization of an original nannofossil ooze) below the hiatus, to grayish yellow green (5GY 7/2) nannofossil-bearing clay with incipient limonite nodules up to 1 cm in diameter. This last lithology, the lowest recognized in Unit II, constitutes the least calcareous part of the Cenozoic sequence, with only ~3% CaCO₃, and rests unconformably on the limestones of Unit III; the contact was encountered in the core catcher of Core 544A-12.

Discussion: The Fe–Mn crust and micromodules, along with an abundance of glauconite and local recrystallization of nannofossil ooze, point to periods of slow deposition during the accumulation of Unit II in a pelagic environment, once again above the foraminiferal lysocline. The color, grayer than Unit I, suggests a more poorly oxygenated sediment profile.

The unconformity at the base of Unit II can be explained either by submarine erosion before the early middle Miocene or simply by nondeposition. We favor the former, because a widespread phase of pre-Miocene erosion has been recognized on the western and eastern North Atlantic margin (Tucholke and Vogt, 1979; Jansa et al., 1979; Lancelot and Winterer, 1980; and von Rad, Ryan, et al., 1979).

Unit III: 103.8 to 139.2 m; Sample 544A-12, CC to 544A-17-1, 23 cm

Unit III consists of 35.4 m of mainly pale reddish brown (10R 5/4) limestone with pale yellowish brown (10YR 6/2) and yellowish gray (5Y 7/2) mottling. The pale reddish brown coloration is probably due to finely dispersed hematite.

The top of the unit was encountered in the core catcher of Core 544A-12, and there was a distinct decrease in drilling rate after about 2 m of penetration into sediments of this core. The upper limit is therefore placed at 103.8 m below the seafloor. Although recovery in Cores 13 to 15 was moderate (50–60%), poorer recovery below this level makes the position of the lower boundary less clear. The marked drop in recovery and an associated higher penetration rate in Core 544A-16 suggests a lithological change even though no rock type other than limestone was recovered. Only the core-catcher sample was recovered for Core 544A-17; this consists of 23 cm of limestone fragments above 4 cm of red sandy clay (Unit IV). The higher penetration rate in Cores 544A-16 and 544A-17 was maintained in 544A-18, yet still only 13 cm of limestone pebbles were recovered, with some reddish clay. A limestone pebble sitting in red sandy clay was similarly encountered at the top of Core 544A-19. We suspect that the major lithological break to Unit IV occurs in Core 544A-16 and that the limestone recovered in the core catchers of Cores 544A-17 and 544A-18 and at the top of 544A-19 represents fragments caved from higher levels. However, the possibility remains that the basal part of Unit III contains unrecovered argillaceous beds (of a different facies to those of Unit IV) and for this reason we place the contact at 544A-17-1, 23 cm, at a depth of 139.2 m below the seafloor.

The limestones of Unit III are dominantly oncoid skeletal intraclast wackestones with subordinate patches of grainstone and packstone. The matrix of the wackestones and packstones is micrite and silt-sized micritic peloids. Grainstones were initially cemented by stubby calcite which rims the grains; this was followed by a blocky calcite pore-filling cement. Echinoderm fragments are heavily overgrown by syntaxial calcite. The internal sediment of the frequent cavities (Fig. 6) is composed of microspar which contains rhombs of overgrown debris of echinoderm cement. Skeletal, oncoid wackestone and packstone become richer in intraclasts downward, where wackestones and packstones with pebble-sized intraclasts are associated with features like stromatolites that show a silt-sized peloidal fabric with irregular laminae that form domal structures in some places. Pieces of the fabric comprise some of the intraclasts, which are mostly of skeletal wackestone. At some levels these intraclasts and the oncoids are intensely limonitized.

Although the limestone color is dominantly pale reddish brown (10R 5/4), pale yellowish brown (10R 6/2), and yellowish gray (5Y 7/2), mottling occurs throughout, and yellowish orange colors tend to be more abundant basally, where a few poorly indurated horizons were encountered.

A thin-shelled, pelagic mollusk similar to *Bositra* of the Tethyan pelagic limestones is abundant; above Core 15 it commonly forms the cores of coated grains. A nektonic assemblage of small though mature ammonites is accompanied above Core 14 by the planktonic *Protoglobigerina* and a moderately diverse benthos (Fig. 7). Conspicuous among the latter are *Pentacrinites*, ostracodes, cerithioid and other gastropods, and vagile foraminifers such as miliolids and nodosariids (*Lenticulina* spp.), but rhynchonellid brachiopods, hexactinellid

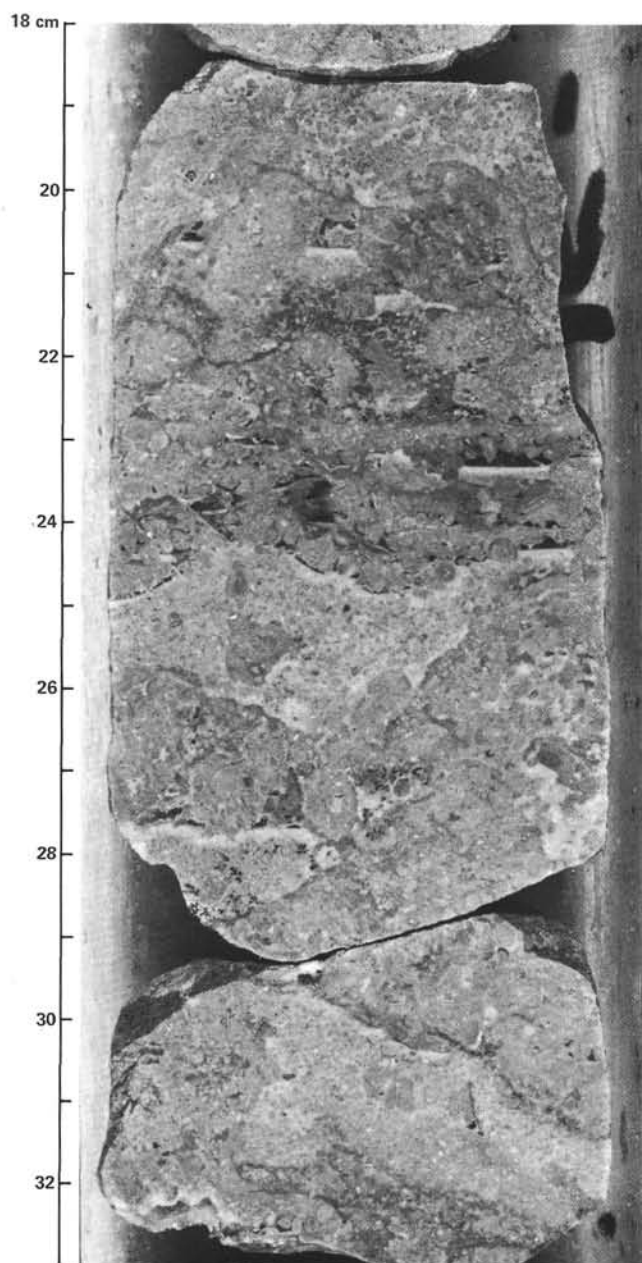


Figure 6. Cavities floored by internal sediment and filled by sparry calcite cement, Sample 544A-15-3, 18–33 cm.

sponge fragments, serpulids, bryozoans, and a solitary coral were also recovered. Bivalve fragments are common, but only one valve, belonging to the genus *Grammatodon*, could be reliably identified. Mechanical abrasion does not appear to have been extreme; a whole cidaroid (echinoid) test was observed in 544A-15-2, 14 cm, and many of the rhynchonellids, ostracodes, and bivalves are articulated. Short strings of connected crinoid ossicles are common. Biological abrasion, on the other hand, is severe, with extensive microborings of skeletal debris. Bioturbation of the limestones is demonstrated by a “churned” fabric and the random orientation of bioclasts (Fig. 8).

Particularly notable is the occurrence of hardgrounds. These show a complex history of formation (Fig. 9):

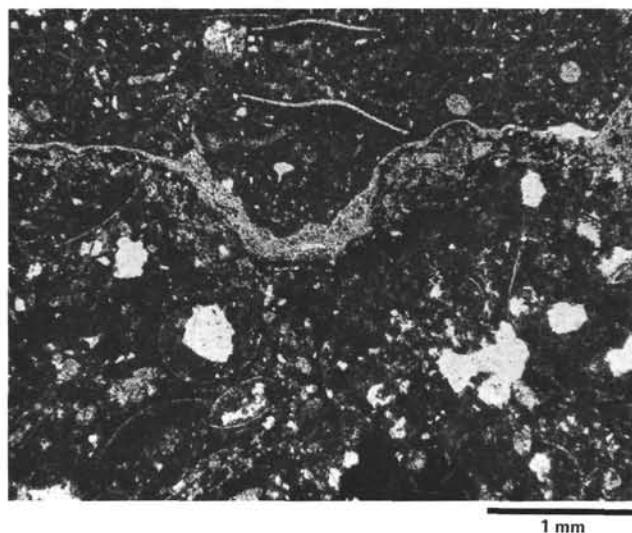


Figure 7. Jurassic skeletal wackestone, rich in filaments (*Bositra*), juvenile ammonites, foraminifers (nodosariids, *Paalzowella*, miliolids), echinoid spines, and ostracodes. The components are frequently micrite-coated. A solution hardground is marked by a Fe–Mn crust and a thin layer of sparry calcite. Sample 544A-13-1, 22–27 cm.

1. Burrowing of a sediment which was firm enough to prevent immediate collapse. (There are no truncated grains indicative of lithification by this stage.)

2. Lithification of the carbonate sediment during a period of nondeposition. An Fe–Mn crust was formed, coating not only the hardground surface, but also the burrow walls, and penetrating well within the surrounding sediment. Erosion and dissolution of the hardground surface occurred locally.

3. Encrustation of the nondeposition surface by serpulid worms.

4. Resumption of sedimentation, which caused only partial filling of the lithified open burrows, leaving voids to be filled later by coarse, sparry calcite.

Proven hardgrounds, as well as other sharp lithological breaks with occasional limonite concentrations that may be incipient hardgrounds, probably mark nondepositional surfaces.

In addition to the sparry-calcite-filled vugs associated with hardground surfaces, spar-filled cavities occur throughout Unit III and toward the base partially retain their original porosity. They are commonly subparallel to bedding and floored by micritic sediment (geopetal fabric; common in the upper part of Fig. 6). At many places these sparry-filled cavities pass laterally into vaguely defined grainstone pipes; they also contain grains fallen from the cavity roofs and walls.

Discussion: The presence of algal-, foraminifer- and serpulid-coated grains and the occurrence of mollusk, gastropod, echinoid, bryozoan, and serpulid debris, all in a micritic matrix, represent deposition in a low-energy, possibly neritic environment. Pelagic fossils, such

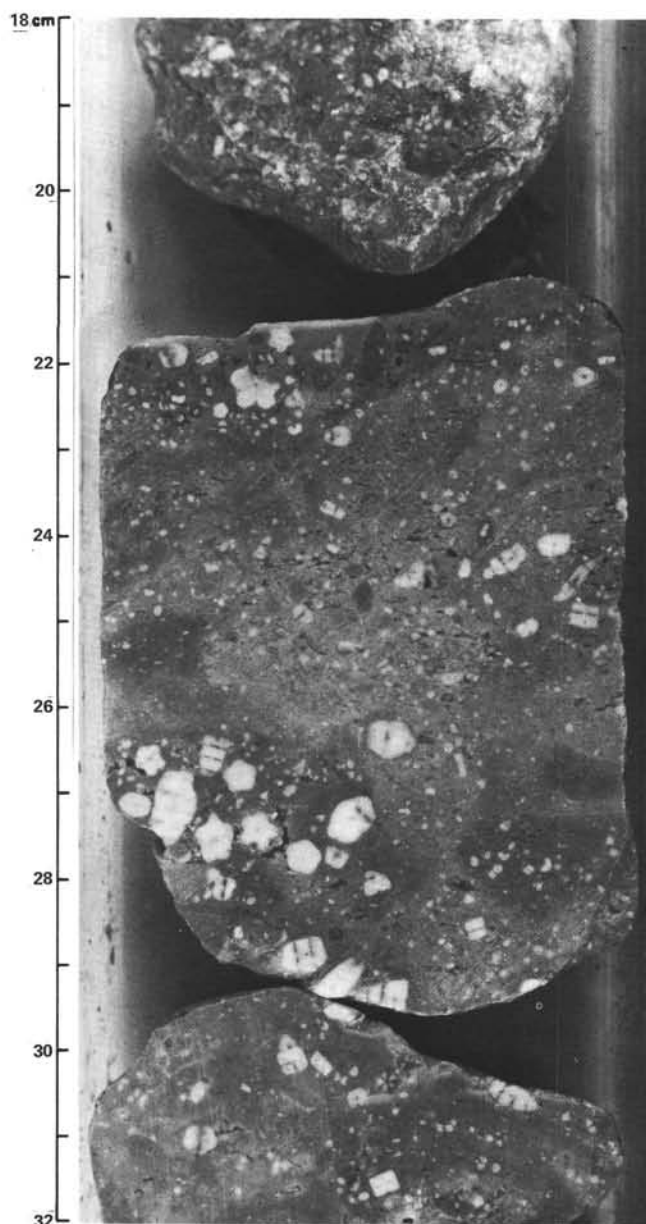


Figure 8. Skeletal (*Pentacrinites*) wackestone showing loosely packed patches caused by bioturbation. Sample 544A-14-1, 18–32 cm.

as thin-shelled bivalves and protoglobigerinids, and the lack of terrigenous clastics suggest an outer carbonate platform setting. The reddish coloration and hardgrounds reflect slow, intermittent deposition. Syndimentary lithification also accounts for the preservation of cavities, which have a complex diagenetic history of filling by internal sediment and micrite, and later void filling by sparry calcite.

Unit IV: 139.2 to 184.3 m; Cores 544A-17-1, 23 cm to base of Core 544A-23

Unit IV consists of 45.1 m of dominantly reddish brown calcareous and variably sandy muds and mudstones, and friable, muddy sands and sandstones. We recognize three subunits.

1. Subunit IVA: muddy sands and sandy muds displaying poorly defined lamination, interlayering, “wispy” bedding, soft-sediment deformation structures and possibly bioturbation;

2. Subunit IVB: sandy mudstones and mudstones with pervasive color mottling and offset microfractures; and

3. Subunit IVC: friable, gravelly-muddy, coarse-grained sandstone and muddy breccia.

The upper boundary of Unit IV is placed at 544A-17-1, 23 cm (but see our comments for Unit III above); the base of the unit rests on gneissic basement between the gravel in Core 544A-23 and the top of Core 544A-24. A change in drilling rate near the top of Core 23 suggests that the top of the basement is at 184.3 m, just under the gravels.

Subunit IVA

Subunit IVA, 27.8 m thick, extends from 544A-17-1, 23 cm to 544A-21-1, 100 cm. The lower boundary occurs at a clear break in recovery within a core where only 215 cm of the 9.0 m penetrated was recovered; hence the contact might be sharp or might be gradational over several meters. Dominantly grayish red (10R 4/6) to moderately reddish orange (10R 6/6) calcareous sandy mud (30%) and muddy sand (70%) compose Subunit IVA, which also contains subordinate layers, wisps, spots, and mottles of gray olive (10Y 9/2) to pale olive (10Y 6/2).

Carbonate bomb analysis reveals up to 18% carbonate (only one sample is as low as 4%), that occurs mostly as crystal aggregates of calcite. The sand fraction is very poorly sorted and variably composes 39–60% of the sediment; concentrations in 5-mm to 20-cm-thick layers occur throughout, increasing in abundance downward. Quartz, ranging in size from very fine sand to granules, is the dominant constituent (about 70%), accompanied by feldspar (about 25%) and carbonate (1–10%); grains are angular to subrounded and compact to compact-elongate. ?Ilmenite, mica, and ?sphene are present as minor constituents. An increase in sand grain size downward is accompanied by increased angularity, an increased feldspar/quartz ratio, and a decreased proportion of limestone fragments. Composite granules of quartz, feldspar, and biotite also occur near the base. The greener layers of Subunit IVA tend to be richer in sand.

Lithoclasts of red and green mud occur throughout the subunit. These are mostly stretched and flattened parallel to bedding, but several are intact, well-rounded clasts up to 4 cm in diameter. Soft-sediment deformation features are common throughout and include disturbed laminae and compacted clasts, isolated patches and wisps of muddy sand, overturned folded layers, and possibly load structures. Structures resembling bioturbation were observed, but these structures might merely result from soft-sediment deformation or root modeling.

Locally, very pale orange (10YR 8/2) and moderate reddish orange (10R 6/6) layers and elongate patches or nodules of micrite (1 m to 2 cm in diameter) lie subparallel to bedding, and crosscut sand laminae in some places. Threefold postformational compaction of the sur-

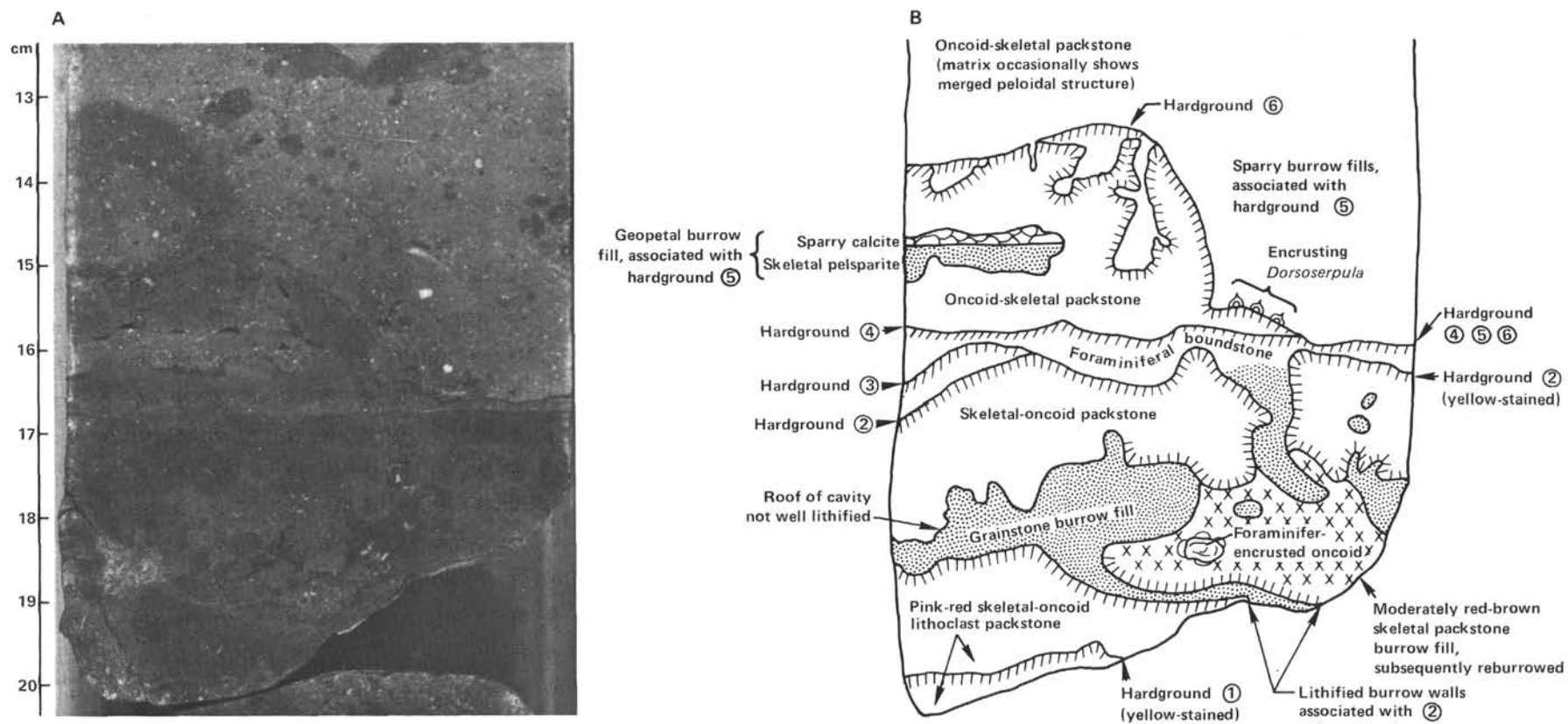


Figure 9. A. Photograph of Sample 544A-13-1, 13-20 cm. B. Sketch of hardground succession shown in A.

rounding sediment (estimated from the distortion of layers and laminae around the nodules) attests to the early diagenetic origin of the nodules. Hematite-limonite crusts and stringers also crosscut laminae and occur as small blebs.

Subunit IVB

This subunit, nominally 8.6 m thick, occurs between 544A-21-1, 100 cm and 544A-22-1, 55 cm.

Though recovery in Core 544A-22 was low (about 1%), the contact of Units IVB and IVC, an abrupt gradation over 6 cm, was preserved. The subunit is dominated by grayish red (10R 4/2) to reddish orange (10R 6/6) sandy mudstone (35%) and mudstone (65%) with pale olive (10Y 6/2) to gray olive (10Y 4/2) mottles, stringers, and patches. Clays are mostly illitic with some kaolinite (from shipboard studies). Sand content ranges from 5 to 15% and is fine to very coarse grained, mostly subangular to angular, and dominated by quartz and feldspar with minor gneiss fragments. This sand occurs mostly as "floating" grains and local sandy mudstone patches.

Subunit IVB is highly fractured and along the fractures finely crystalline pink calcite is concentrated. Reduction of the red iron oxide have resulted in spots, halos, and stringers of pale olive in the surrounding sediment. Later offsetting of the fractures has produced a "microfracture" texture throughout the mudstone.

Subunit IVC

This subunit, nominally 8.7 m thick, extends from 544A-22-1, 55 cm to the base of the gravel in Core 544A-23.

Recovery of less than 5% in this interval makes the thickness suggested at best approximate. The subunit is composed mainly of grayish red (10R 4/2), grain-supported but very poorly sorted, pebbly-muddy sand, muddy-sandy gravel, and muddy breccia (Fig. 10). Grains are angular to very angular and composed of quartz, feldspar and weathered gneissic fragments. The largest grains are the size of small cobbles (Fig. 11), and a few show a more strongly foliated fabric than the underlying basement. The mud at the base of the unit has characteristics of fine-grained breccia with muddy matrix. A fining-upward trend within Subunit IVC was accompanied by decreasing angularity of the clast components.

Discussion: Unit IV contains characteristics of continental deposits formed on a low-relief gneissic terrain in a humid climate. The very poorly sorted, highly angular, weathered gneiss clasts in a muddy matrix within Subunit IVC were formed as a colluvium-alluvium blanket on the underlying metamorphic basement. This unit shows no evidence of transport. All the lithic clasts are weathered and range widely in size. The grain size increases downward with no increase in sorting and in the relative amount of gneiss clasts. It is clear that the clasts originate from the basement and have not been transported any significant distance.

Overlying Subunit IVC, IVB contains characteristics of a humid paleosol. Quartz and feldspar grains float throughout a highly altered muddy matrix. Stringers and

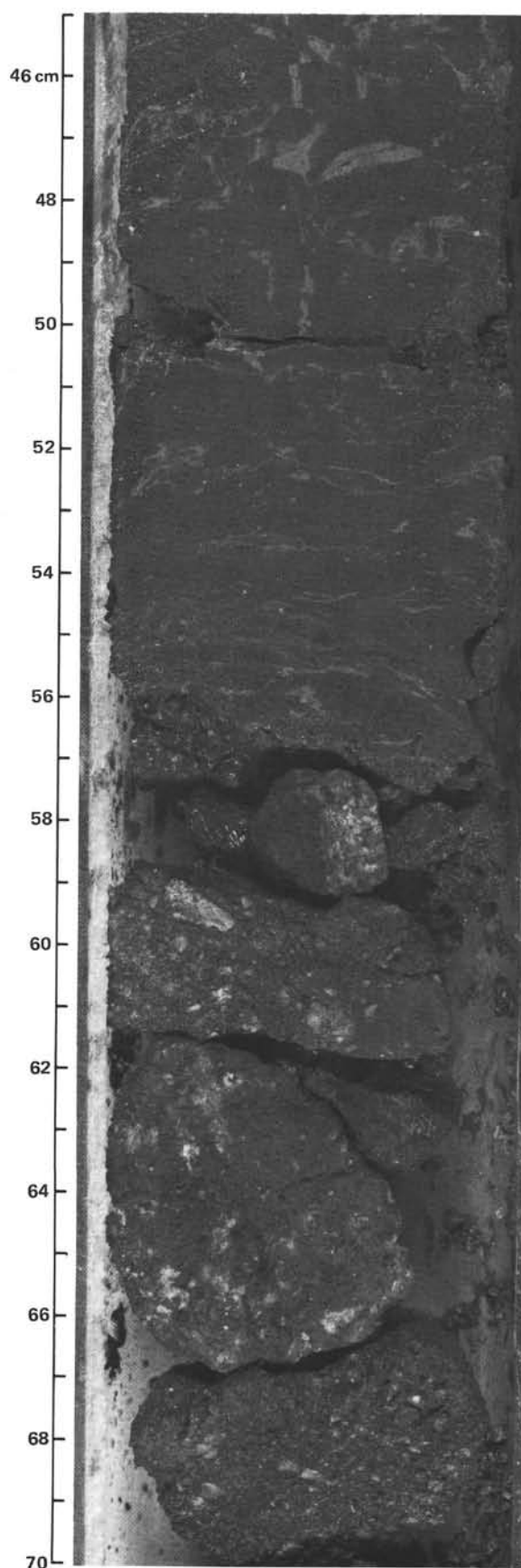


Figure 10. Section 544A-22-1, base of Unit IV: mostly reddish brown sandy mudstone (45–57 cm) and muddy gneissic breccia (57–70 cm).

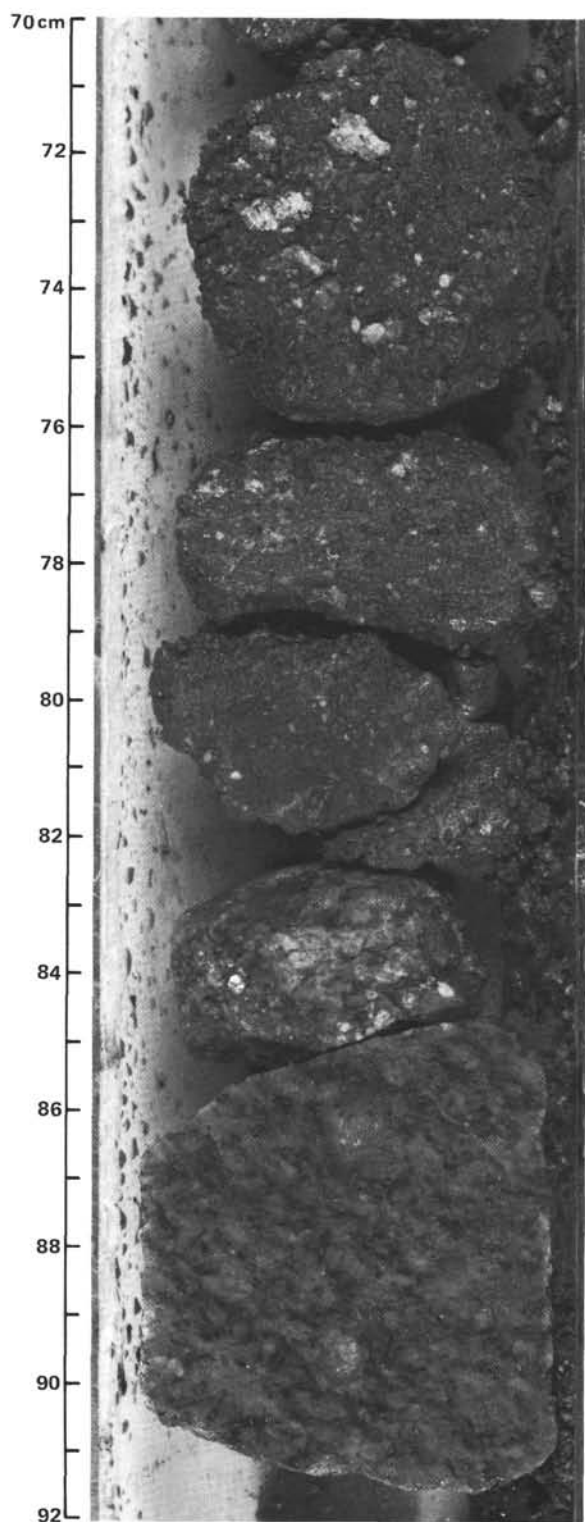


Figure 11. Muddy gravel of Subunit IVC, with a cobble of gneiss identical to the basement rocks of Unit V. Sample 544A-22-1, 70–92 cm.

veins of calcite have pushed apart grains and matrix forming features similar to those in caliches. Once again there is no evidence of sorting or transport.

Subunit IVA shows features indicative of transport and rapid deposition by mud flows. The percentage of

sand and granules is greater than in IVB; they are concentrated in patches and stringers. Soft-sediment deformation features abound, as do flattened and stretched mud clasts. Mud flows reworking the deposits of IVB could easily form the textures and structures in IVA. Such flows would have been mud-dominated, with only minor associated channel or sheet flow to concentrate and sort sand and granules. Some of the turbation in IVA may be due to intense root bioturbation as plants colonized the fresh mud flow, but most is due to plastic deformation during and immediately after deposition.

All these deposits probably formed in a humid environment in a low-relief terrain, which resulted in deep weathering of the metamorphic basement and formation of thick, clay-rich soils. This large amount of clay was the source for the mud flows that overlie alluvial and paleosol deposits.

Unit V: 184.3 to 235.0 m, T.D.; Cores 544A-24 to 544A-28

The reddish sandy clays of Unit IV rest on a pinkish gray biotite-bearing gneiss which was penetrated to a total thickness of 50.7 m. Partial alteration of biotite to hematite was observed throughout the section. Hematite stains a well-developed joint set oriented about 80° to the foliation, as well as a more diffuse system of microfractures.

The physical contact with the overlying conglomerates of Unit IV was not recovered but lies between Cores 23 and 24, most likely at a depth of 184.3 m. Microscopic study of crystalline basement rocks, based on preliminary examination aboard ship of thin sections from Samples 544A-24-1, 39–42 cm and 544A-25-1, 35–39 cm, describe strong wavy foliation, marked by layers of mica and of stringy quartz wrapped around blocky feldspars. Most grains show strong signs of strain such as wavy extinction, bent twins, or cracks. The quartz is most severely deformed, being stretched out in long lenticular grains that tail off into stringers of crushed (and recrystallized) grains. The foliation is subhorizontal in all cores recovered. The composition of Unit V sediments is as follows:

1. Plagioclase (60–70%) is generally zoned (mainly progressive, but some oscillating) and of negative optical sign, suggesting intermediate composition. The inner parts of the zoned crystals are strongly altered and cloudy, with abundant small sericite flakes along cleavages.

The largest plagioclase grains are about 2–3 mm across with generally clear outer zones. Twins are common and bent. Some grains contain broken K-feldspar (10%), mainly orthoclase, but some microcline. The plagioclase is commonly perthitic, generally clear or slightly altered. Smaller plagioclase grains (mainly about 1 mm) are also common.

2. Quartz (20%), in long stringers, with much wavy extinction, wraps around feldspars and is fractured at the contacts and at the ends of the quartz lenses. Zircon is common as inclusions, especially in the crush zones.

3. Mica (5%) as muscovite is bent around feldspars; biotite (trace) is also bent, but is very altered to opaque

and red brown (Fe_2O_3 ?). Some flakes look chloritic, but the alteration prevents certain identification.

This rock is a cataclastic "augen" or "flaser" gneiss, and probably had an intermediate igneous rock protolith—perhaps a quartz monzonite or quartz diorite.

Hole 544B

Hole 544B was piston cored to a depth of 39.3 m below the seafloor. There is only one lithologic unit, which is compositionally identical to Unit I in Hole 544A.

Unit I: 0 to 39.3 m

The sediment cored in Hole 544B is mainly pale yellowish brown (10YR 6/2), clayey foraminifer nannofossil ooze, which is early Pleistocene to late Miocene in age.

Accessory mineral components of the oozes are subangular detrital quartz grains (low to max. 5%), dolomite rhombs (low to max. 2%), pyrite balls and cubes (low to max. 10% in dark gray blebs) and plates of muscovite.

Because the HPC was used, the cores generally show little or no drilling disturbance. Color bedding (Cores 544B-7 and 544B-8) often displays fine color laminations (Cores 544B-2 and 544B-4), from dark yellowish brown (10YR 4/2), grayish orange (5YR 7/4), grayish orange pink (5YR 7/2) to pinkish gray (5YR 8/1) and light brown gray (5YR 6/1), with fine (2–5 mm) intercalations of dark gray layers (increasing content of pyrite, Zone N3). In Core 544B-4, a greenish glauconite layer is visible.

Color mottling and the tubelike, slightly flattened spots of lighter or darker color were generated by bioturbation by burrowing organisms.

Discussion: Hole 544B was drilled at the same location as Hole 544A but was hydraulic piston cored to obtain undisturbed cores for geomagnetic, biostratigraphic, and isotopic studies. Thus the discussion of Hole 544A is applicable to Hole 544B.

BIOSTRATIGRAPHY

Biostratigraphic Summary and Synthesis

The main objective of Site 544 (MAZ-3) was to reach mid-Mesozoic strata and possibly crystalline basement rocks known from piston coring near the site (Wissmann and von Rad, 1979). Depending on the drowning and submarine-high history of this small area, the drill was expected to penetrate a highly reduced sedimentary column including major stratigraphic hiatuses, exceeding in frequency and time value those previously drilled at Sites 370, 416 and 415 (Lancelot and Winterer, 1980). The 184 m of sedimentary strata drilled in Hole 544A represents the total column from the Pleistocene to the top of the crystalline basement. Two minor hiatuses were detected within the Cenozoic sequence, and three very major gaps do occur: between the Cenozoic and the Jurassic carbonate rocks; between these and the possibly late Triassic–Early Jurassic red sandy mudstones; and at the contact between the sedimentary series and the basement.

The interval from Core 544A-1 through Section 544A-7-1 (and 544B-1 through 544B-12) represents a nearly continuous early to middle Pleistocene to late Miocene sequence that is rich in nannofossils and foraminifers but lacks any determinable siliceous forms except traces of sponge spicules in Core 1. Shipboard age determinations based on nannofossils and foraminifers correspond very well in Hole 544B (HPC) but significant discrepancies exist between the two microfossil groups in the upper part of Unit I of Hole 544A owing to the severe drilling disturbance. Within Core 544A-7, between Samples 544A-7-1, 105–107 cm and 544A-7-3, 115–117 cm, a hiatus (or condensed sequence?) is documented by late Miocene (N17) foraminiferal assemblages less than 10 cm above a middle Miocene (N14) fauna. The interval from 544A-7-3 through 544A-12-1, 60 cm represents the middle Miocene (N14 to N9), characterized by scarce foraminifers and traces of undeterminable radiolarians in the upper part.

Another hiatus is recorded by a glauconite-rich layer in 544A-12-1, 60–74 cm, which contains early Miocene (N7) foraminiferal assemblages. The base of the Cenozoic section, still early Miocene (N7) in age, can be nominally placed in Sample 544A-12, CC, where a piece of Jurassic limestone was recovered at the very bottom of the core.

Cores 544A-13 through 544A-18 contain yellow and red skeletal intraclast peloid limestones.

The contact between the limestone and the underlying unit was not sufficiently well recovered to allow any genetic interpretation. However, the totally different environmental situation of the two units (see sediment lithology section of this chapter) suggests a hiatus between the limestones and the formation beneath.

The interval from 544A-17-1, 23 cm through 544A-21-1, 100 cm contains dominantly reddish brown sandy mudstones and muddy sandstones which are completely barren. In analogy with the red beds of Site 547, this unit might be of ?Rhaetian–Sinemurian age. The red mudstones rest with an intervening thin breccia on gneiss. In comparison to the Moroccan Meseta, this gneiss may be of early Paleozoic age.

Nannofossils

This report will combine results from the three holes at Site 544 to give a more continuous representation of the nannofossils present.

Core 544-1 contains calcareous nannofossils of the *Emiliania huxleyi* Zone (NN21) (Gartner, 1977), which is of late Pleistocene age. The assemblage consists of *Emiliania huxleyi*, *Gephyrocapsa* spp., and *G. oceanica*; *Pseudoemiliania lacunosa* and *Calcidiscus macintyreii* are also present but are considered reworked. The zone is defined by the first appearance of *E. huxleyi*, which is quite small; further investigation is needed with a scanning electron microscope. The assemblage in Core 544A-1 is of moderate to good preservation and common abundance; it contains and forms as *C. macintyreii*, *P. lacunosa*, *G. caribbeanica*, *G. oceanica*, and *Coccosphaera leptopora*. The presence of *Calcidiscus macintyreii* and *P. lacunosa* is explained by reworking of older sediments, because the site is located upon a slope.

Cores 544B-1 through 544B-3 contain a similar assemblage; further work with the scanning electron microscope will determine whether *E. huxleyi* is present or not in these samples.

Cores 544A-2, 544B-4, and 544B-5 consist, in part, of *Discoaster brouweri*, *C. macintyreii*, *Helicosphaera kamptneri*, *P. lacunosa*, and *Coccosphaera leptopora*. This assemblage is placed in the *D. brouweri* Zone, *Calcidiscus macintyreii* Subzone (NN18) (Okada and Bukry, 1980), and is of late Pliocene age. Core 544A-3 is also tentatively classified in this subzone. Preservation is good and abundance common in these cores.

Core 544A-5 could be middle to early Pliocene in age, because no determining markers have been found. The assemblage consists partly of *Reticulofenestra pseudumbilica*, *D. berggrenii*, *D. brouweri*, *Amaurolithus primus*, and *C. macintyreii*; preservation is good and abundance is common.

Cores 544B-6 through 544B-10 are assigned to the *A. tricorniculatus* Zone (NN12-13/14) (Okada and Bukry, 1980), which is of early Pliocene age. A representative assemblage is *A. tricorniculatus*, *A. primus*, *D. brouweri*, *D. variabilis*, *R. pseudumbilica*, and *D. surculus*. Abundance is quite high and preservation is good.

In the Pliocene section, a substantial portion of the middle and late Pliocene is absent in Holes 544A and 544B. There is no visible hiatus or lithology change to accompany this considerable break in the nannofossil record.

The nannofossils contained in the interval from 544A-5 through 544A-7-1, 50-51 cm are of late Miocene age, as are those in Cores 544B-11 and 544B-12. The assemblages are of the *D. quinqueringus* Zone (NN11) (Okada and Bukry, 1980) and contain, in part, *D. quinqueringus*, *D. brouweri*, *A. delicatus*, *A. primus*, *D. variabilis*, *D. pentaradiatus*, and *C. macintyreii*. Abundance in both holes was common, preservation moderate to good.

The exact age of the section from 544A-7-2, 50-51 cm through 544A-9-2, 130 cm could not be determined by nannofossils, since no marker species could be recognized. The age could range between late and middle Miocene; a representative assemblage is *C. macintyreii*, *D. variabilis*, *R. pseudumbilica*, *D. exilis*, *D. challengerii*, *D. braarudii*, and *C. leptopora*. Species abundance in these cores ranges from few to common; preservation is generally moderate. Dissolution may be a factor because the hardy *Coccolithus*, *Discoaster*, and *Calcidiscus* are present, but many of the markers in this interval are discoasters; a hiatus may exist in this section.

The interval from 544A-9-4, 4 cm through 544A-10-2, 87-88 cm contains an assemblage that belongs in the *Sphenolithus heteromorphus* Zone (NN5) or *D. exilis* Zone, *Coccolithus miopelagicus* Subzone (NN6) (Okada and Bukry, 1980). The age of this interval is early middle Miocene; the assemblage consists, in part, of *Calcidiscus macintyreii*, *Cyclicargolithus floridanus*, *D. exilis*, *D. variabilis*, *Coccosphaera leptopora*, and *D. braarudii*. Preservation is moderate to good, with abundance common.

The interval from 544A-10-2, 87-88 cm to 544A-12-1, 4 cm is contained within the *S. heteromorphus* Zone (Okada and Bukry, 1980) (NN5) and is of early middle

Miocene age. A representative assemblage is the same as the one from the section above except for the inclusion of *S. heteromorphus*; preservation in this interval is good and abundance common. Below this, from 544A-12-2, 16 cm to 544A-12, CC, the boundary fossils are absent; only *Calcidiscus macintyreii*, *D. variabilis*, *R. pseudumbilica*, and *Coccolithus pelagicus* remain. This interval could also be early middle Miocene, though no markers are seen. Dissolution may have been a predominant factor, since only hardy genera survived; preservation is poor to moderate, species few to rare in abundance.

In Sample 544A-14-1, 120 cm, a single *Stephanolithon bigotii* was possibly observed; this identification is tentative owing to the small size of the specimen and several obscuring clay particles, and an SEM or more powerful light microscope must be used for better results. The range of *S. bigotii* is from the lower Callovian to middle Kimmeridgian.

Neogene Foraminifers

The composite Neogene section of Site 544 is represented by Pleistocene through early Miocene foraminiferal nannofossil ooze (sedimentary Units I and II); it rests unconformably on Jurassic limestone (Unit III). Two minor hiatuses are recognized in the Neogene sequence, one between the late and middle Miocene and the other between the middle and early Miocene. Both are associated with glauconite-bearing sediments. The biostratigraphic zonal scheme followed for the Cenozoic is from Stainforth et al. (1975).

The Pleistocene is represented by the *Globorotalia truncatulinoides* Zone (N22-23). Common planktonic taxa are *G. truncatulinoides*, *G. hirsuta*, *G. scitula*, *G. crassiformis*, *G. inflata*, *Orbulina universa*, *Globigerina bulloides*, *G. glutinata*, *Globigerinoides conglobatus*, *G. ruber*, *G. trilobus*, with rare *Neoglobobulimina pachyderma*. Benthics include *Buliminidae*, *Miliolidae*, *Nodosariidae*, *Textularia* spp., *Cibicides* spp., *Melonis* spp., *Eponides* spp., and *Pullenia* spp.

The late Pliocene *Pulleniatina obliquiloculata* Zone (N20-21) is characterized by *P. obliquiloculata*, *Orbulina universa*, and *Sphaeroidinella dehiscens*. Other common planktonics include *Globorotalia crassiformis*, *G. inflata*, and *Globigerina bulloides* with rare *G. venezuelana* and *Globorotalia acostaensis*. Benthic species similar to those of the Pleistocene are noted in this zone.

The *Globorotalia margaritae* Zone (N18-19) encompasses the middle to early Pliocene. The characteristic planktonics include *Globorotalia margaritae*, *G. cf. plesiotumida*, *G. acostaensis*, *Globigerina nepenthes*, *Sphaeroidinellopsis subdehiscens*, *Globoquadrina altispira*, and *Orbulina universa*. The genus *Uvigerina* is a conspicuous member of the benthic fauna.

Species characteristic of the late Miocene *Globorotalia acostaensis* Zone (N17) include *G. acostaensis*, *G. juanai*, *G. plesiotumida*, *Globigerina nepenthes*, *Globoquadrina dehiscens*, *G. altispira*, *Sphaeroidellopsis seminulina*, *S. subdehiscens*, and *Orbulina universa*. Benthic faunas are common and diverse.

The upper *Globorotalia acostaensis* Zone corresponds to the Messinian Stage and represents a deep, open-ocean

record of the salinity crisis of the Mediterranean Sea at the end of the Miocene. The foraminiferal content of the ooze is significantly lower in the late Miocene sequence. Here the late Miocene (N17) rests unconformably upon middle Miocene (N14) foraminiferal nannofossil ooze. Across this hiatus, the drop in foraminiferal content from middle to late Miocene is sharp. There is a gradual increase in foraminiferal content across the Miocene/Pliocene boundary. Such a trend clearly indicates that the Messinian salinity crisis had an effect on the marine carbonate system.

As mentioned above, a stratigraphic hiatus is observed between late Miocene (N17) and middle Miocene (N14) sediments. The break occurs in Core 544A-7, possibly associated with the glauconitic nannofossil ooze of Section 2. Samples 544A-7-1, 105–107 cm and 544A-7-3, 115–117 cm are late Miocene and middle Miocene, respectively.

The middle Miocene *Globorotalia siakensis* zone (N14) is represented by the interval 544A-7-3, 115–117 cm. Below this, to Core 544A-10, the middle Miocene zones were not clearly distinguished during shipboard examination and so are lumped as N10–14. Planktonic species characteristic of this interval include *G. siakensis*, *G. praemenardii*, *Globigerinoides trilobus*, *Orbulina universa*, *Sphaeroidinellopsis seminulina*, *Globoquadrina dehiscens*, *G. altispira*, and rare *Globigerina venezuelana*.

Foraminifers recovered from 544A-10, CC and 544A-11, CC indicate an early middle Miocene age (N9–11) because of the co-occurrence of *Globigerinoides sicanus* and *Orbulina universa*.

In Core 544A-12, a thin glauconitic bed (544A-12-1, 60–64 cm) marks the boundary of the other minor Neogene hiatus, here separating the middle and early Miocene. A sample from within the glauconitic bed (544A-12-1, 63–64 cm) gives an early Miocene age and represents the lower *Globigerinatella insueta* Zone (N7). The loss of *Orbulina universa* and the presence of *Catapsydrax* cf. *stainforthi* and *Globigerinoides sicanus* establish the late early Miocene position.

Mesozoic Foraminifers and Other Fossils (Hole 544A)

In thin sections cut from Cores 544A-12 to 544A-16, the following forms were seen (F = few, R = rare): ammonites (F), ostracodes (F), echinoderms (fragments; F), lamellibranchs (fragments), gastropods (fragments), bryozoans (fragments), encrusting cyanobacteria.

Foraminifers observed were *Protoglobigerina* sp. (R), *Ammobaculites* sp. (R), *Lenticulina* sp., nodosarids, miliolids (both free and attached, ophthalmitids, and *Protoneroplis* sp. (in a peel only).

None of these organisms or their association allow us to give a precise age. For example, *Protoglobigerina* sp. is known from the Dogger to the Kimmeridgian.

Washed samples from the red sandy mudstones are completely barren of fossil remains.

DEPTH-VERSUS-AGE CURVE

A condensed Neogene record, 104 m thick, was cored at Site 544 (Fig. 12). The sedimentation rate for the interval from late Miocene to Pleistocene was about 8 m/

m.y. A hiatus spanning about 4 m.y. separates upper Miocene from middle Miocene sediments. The sedimentation rate during the middle and late Miocene, represented by the sediments beneath the hiatus, was also about 8 m/m.y.

ORGANIC GEOCHEMISTRY

The sediment cores recovered at Site 544 lacked any detectable amounts of free hydrocarbon gases. We did not apply carrier gas stripping gas chromatography for light hydrocarbons because the Cenozoic sediments were too poorly consolidated and the Jurassic limestones and underlying sandy muds looked strongly oxidized.

Carbon and Nitrogen Contents

The Cenozoic foraminiferal and nannofossil oozes (Units I and II) are calcareous to highly calcareous but contain only small amounts of organic matter (Table 3). Only a few samples analyzed exceed 0.2% C_{org} , and there is a negative correlation between organic and carbonate carbon content. A correlation coefficient of $r = 0.60$ ($r_{05, 15} = 0.48$) was calculated for the relationship between C_{org} and noncarbonate residue (Table 4). There is a trend of increasing carbonate amount within Unit I ($r = 0.75$; $r_{05, 15} = 0.48$). The organic nitrogen values (Tables 3 and 4) show fairly constant level, but considering the low organic carbon contents the accuracy of the nitrogen values may be low. The Jurassic limestones and the mudstones and sandstones overlying the gneissic basement contain only insignificant amounts of organic matter.

Pyrolysis

Eight sediment samples from the Cenozoic interval of Hole 544A were studied by Rock-Eval pyrolysis to determine the type of organic matter present and its maturity (Table 3). The hydrogen index values are low throughout, although they are slightly higher in the middle Miocene (55 to 139 mg HC/g C_{org}) than in the younger sections (5 to 31 mg HC/g C_{org}). The oxygen index values are extremely high (between 300 and 2700 mg CO_2 /g C_{org}) and do not show any trend with lithologic unit or age. Regarding the low organic carbon and high carbonate contents of the Cenozoic samples, the extremely high oxygen index values seem to indicate partial carbonate decomposition below 390°C, that is, before the CO_2 trap on the Rock-Eval instrument is closed. The chemical composition of the organic matter in the Cenozoic sediments seems to be hydrogen-deficient and highly degraded, characteristics of organic matter deposited in a pelagic environment with an oxidizing water column or after long-distance transport. There is no indication that the pyrolyzable portion of the organic matter is reworked, because the temperature of maximum pyrolysis yield (T_{max}) indicates a low level of maturation throughout (Espitalié et al., 1977; Boutefeu, 1980).

Three samples from the Jurassic limestones (544A-15-3, 102–104 cm) and the underlying sandy mudstones (544A-20-3, 0–2 cm, red color; 544A-20-3, 5–6 cm, green color) did not yield any hydrocarbons upon pyrolysis. This is consistent with the extremely low organic carbon contents (0.01%).

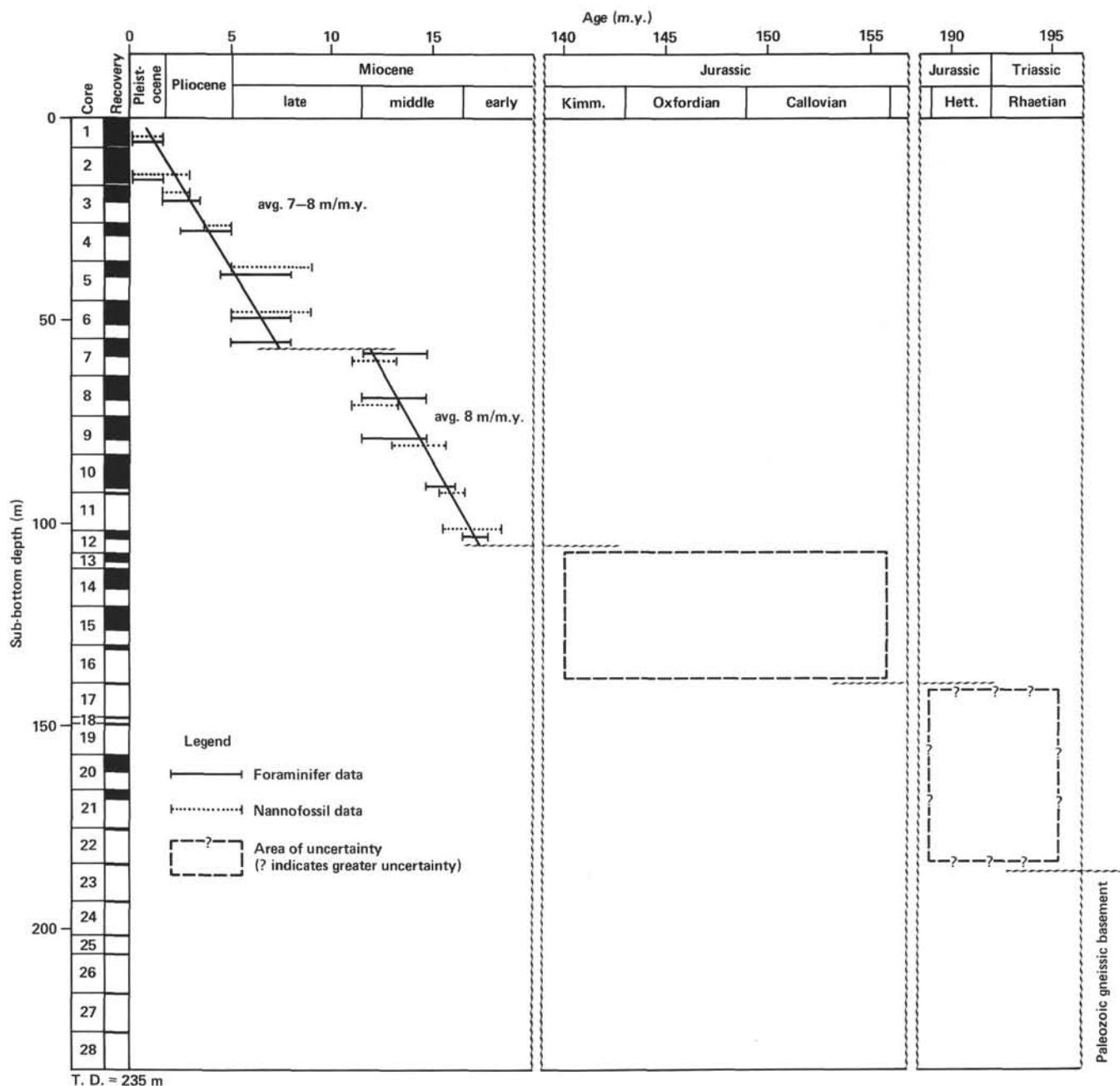


Figure 12. Depth versus age at Site 544 (Hole 544A).

IGNEOUS AND METAMORPHIC PETROLOGY

The description of the metamorphic rocks cored at this site is included in the section on Sediment Lithology, this chapter.

INORGANIC GEOCHEMISTRY

A summary of the inorganic geochemistry data for Site 544 is given in Table 5 and Figure 13.

MAGNETICS

Hole 544A

The nannofossil ooze (Unit I) was highly deformed by the rotary drilling. Oriented samples were collected

from the less deformed sections in order to test their magnetic properties in anticipation of the use of the HPC at Hole 544B.

In Core 7, the abrupt change in color from the upper red-brown ooze (Unit IA) to the lower gray-green ooze (Unit IB) coincides with a change in magnetization intensity. The oozes above the unconformity have natural remanent magnetization (NRM) intensities of 5×10^6 to 1×10^{-6} G, whereas those below have NRM intensities two orders of magnitude lower, below the noise level (10^{-7} G) of the Digico magnetometer.

Three samples from Unit IA were demagnetized stepwise in peak fields up to 800 Oe. The magnetization directions remain consistent during the demagnetization procedure, suggesting the presence of a single magneti-

Table 3. Carbon and nitrogen contents and pyrolysis data, Hole 544A.

Core-Section (interval in cm)	Sub-bottom depth (m)	Litho- logic unit	Age	Rock-Eval pyrolysis								
				C _{Org} (%)	CaCO ₃ (%)	N _{Org} (%)	S ₁ (mg/g rock)	S ₂	S ₃	Hydrogen index (mg HC/g C _{Org})	Oxygen index (mg CO ₂ /g C _{Org})	T _{max} (°C)
1-1, 142-144	1.4	I	Pleistocene	0.10	49.5	0.04						
1-1, 144-150 ^a	1.5			0.07	53.0	0.04						
2-4, 142-144	12.9			0.37	41.3	0.06						
2-4, 144-150 ^a	13.0		Pliocene	0.12	54.3	0.04						
2-5, 118-120	14.2			0.16	57.0	0.04						
2-6, 0-2	14.5			0.08	62.0	0.03	—	0.02	2.05	20	2563	397
4-1, 144-150 ^a	27.5		Miocene	0.11	69.1	0.03	—	0.02	0.80	17	727	397
5-2, 118-120	38.2			0.11	72.6	0.02	—	0.01	1.60	5	1411	402
5-3, 0-2	38.4			0.13	69.6	0.03						
7-1, 130-132	55.8			0.17	61.0	0.04	—	0.05	1.18	31	694	402
8-2, 144-150 ^a	67.0			0.09	77.1	0.02						
8-3, 118-120	68.2			0.11	76.1	0.02	—	0.06	1.60	55	1455	407
8-4, 0-2	68.5			0.19	71.6	0.03						
9-1, 70-72	74.2			0.27	65.0	0.05	—	0.19	1.02	70	378	407
10-2, 80-82	85.3			0.08	66.0	0.03	—	0.11	2.16	139	2700	407
12-1, 37-39	102.4			0.29	58.3	0.05	—	0.29	0.98	100	338	412
12-2, 11-13	103.6	II	Jurassic	0.01	3.1	0.02						
15-3, 102-104	125.0			0.01	100.0	0.01	—	—	—	—	—	—
17-1, 26-27	139.3	III	Jurassic	0.01	11.5	0.05						
19-1, 79-81	150.3			0.01	3.7	0.05						
20-2, 118-120	159.7	IVA	Jurassic	0.01	18.3	0.04						
20-3, 0-2	160.0			0.01	14.1	0.03	—	—	—	—	—	—
20-3, 5-6	160.1			0.01	16.7	0.01	—	—	—	—	—	—

Note: — = not detected.

^a Residues from interstitial water analysis.Table 4. Statistical characteristics of CaCO₃, C_{org}, and N_{org} contents in sediments from Hole 544A.

Lithologic unit	Age	N	CaCO ₃ (%)				C _{org} (%)				N _{org} (%)			
			Range	Mean	Variance	S. D.	Range	Mean	Variance	S. D.	Range	Mean	Variance	S. D.
I	Pleistocene– middle Miocene	15	41.3–77.1	63.0	100.0	10.35	0.07–0.37	0.14	0.006	0.081	0.02–0.06	0.03	1 × 10 ^{−4}	0.011
II	early Miocene	1		58.0				0.29				0.05		
		1		3.1				0.01				0.02		
III	Jurassic	1		100.0				0.01				0.01		
IVA	?latest Triassic to Early Jurassic	5	3.7–18.3	12.9	26.3	5.74	0.01–0.01	0.01	0.0	0.0	0.01–0.05	0.04	0.129	0.017
Total		23												

Note: Mean (\bar{y}) = $\frac{1}{N} \sum_{i=1}^N y_i$; variance = $\frac{1}{N} \sum_{i=1}^N y_i^2 - \left(\frac{1}{N} \sum_{i=1}^N y_i \right)^2$; S.D. = $\sqrt{\text{var} \frac{N}{N-1}}$

Table 5. Summary of shipboard inorganic geochemical data, Holes 544 and 544A.

Laboratory sample no.	Sample (interval in cm)	Sub-bottom depth (m)	pH	Alkalinity (meq/l)	Salinity (‰)	calcium (mmoles/l)	Magnesium (mmoles/l)	Chlorinity (‰)
IAPSO standard seawater								
	Surface seawater		7.62	2.424	35.2	10.55	64.54	19.378
			8.12	2.450	36.8	10.97	56.03	20.362
Hole 544								
1	1-1, 144-150	1.44-1.50	7.29	2.870	35.7	10.710	51.284	19.616
Hole 544A								
2	2-4, 144-150	12.94-13.00	7.24	2.913	36.0	10.991	51.003	19.683
3	4-1, 144-150	27.44-27.50	7.22	2.540	35.8	11.914	48.675	19.582
4	8-2, 144-150	66.94-67.00	7.31	2.203	35.9	13.418	45.766	19.683
5 ^a	12-2, 11-13	103.61-103.63	b	b	36.3	14.963	48.524	19.887
6 ^a	17-1, 26-27	139.26-139.27	b	b	37.1	17.089	50.701	20.226
7 ^a	19-1, 45-46	149.95-149.92	b	b	36.1	b	b	b
8	20-1, 144-150	158.44-158.50	7.34	2.539	36.0	14.301	48.747	19.853
9	21-1, 147-150	167.47-167.50	b	b	36.4	14.481	50.059	20.023

^a Sample taken after core was split open in the core lab for salinity monitoring.^b Not enough sample to perform these analyses.

zation component. Median destructive fields of about 200 Oe indicate the absence of high coercivity contributors to the remanence.

The pale red-brown limestones from Cores 12-16 were sampled, wherever the correct orientation upward of core fragments was unambiguous. The NRM intensities generally range from 5×10^{-7} G to 5×10^{-6} G. The

results from these limestones are given in Channell (this volume).

Hole 544B

Results from the HPC were disappointing for a number of reasons. First, the plastic core liners of Cores 3, 4, 5, and 6 cracked during coring, distorting and deform-

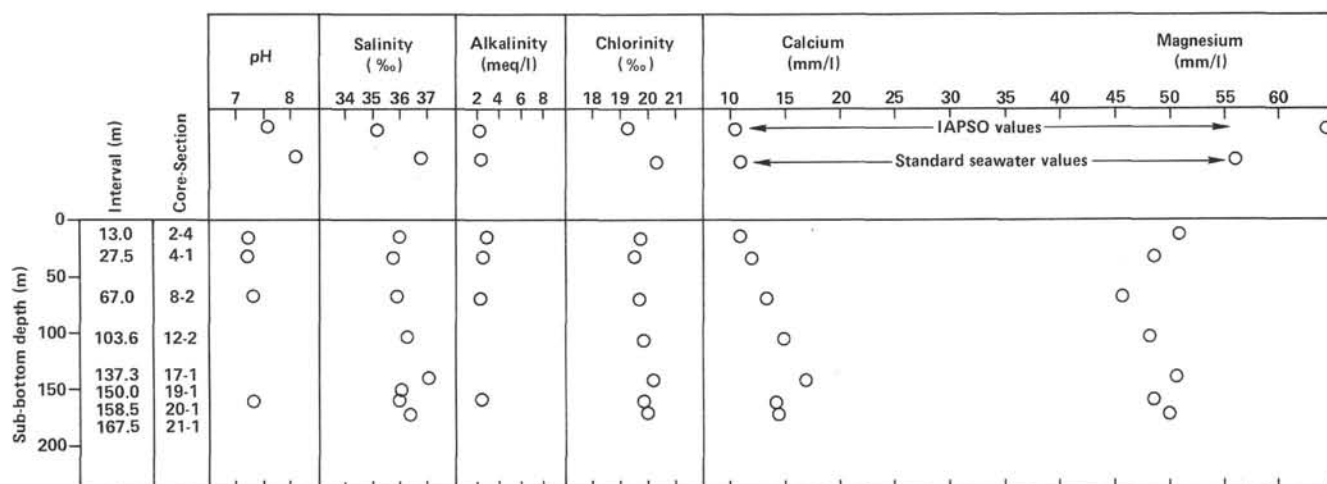


Figure 13. Interstitial water chemistry, Hole 544A.

ing the sediment. Secondly, a viscous remanent magnetization (VRM) affected all cores, especially Cores 9 to 12.

Each sample was AF demagnetized at a number of stages in order to ascertain its characteristic magnetization. The magnetization directions usually remain stable during demagnetization. The characteristic magnetizations are plotted as a function of depth in Figure 14. The inclination data from Core 1 are very scattered, probably because of drilling disturbance. The data from Cores 2 to 8 give a more consistent picture but the large gaps because of unsampled (deformed) core do not allow unambiguous correlation of polarity zones with the Pliocene-Pleistocene reversal time scale.

The NRM intensities increase sharply below Section 544B-9-2, and the NRM declinations become very consistent between sections, suggesting remagnetization after coring.

A simple test was carried out to investigate the extent to which these sediments can acquire VRM. One sample from each core was demagnetized in a peak field of 600 Oe. The samples were then immediately placed on an inclined surface so that one of the orthogonal sample orientation directions (the X direction) coincided with the ambient magnetic field in the laboratory. The magnetization intensity (in the X direction) was then measured after three increments of log (time), after 1, 4, and 13 hr. VRM is rapidly acquired by most samples. It seems likely that severe VRM overprint spoils the NRM signal from many of the samples, especially from Cores 9-12, where this VRM has very high coercivity. Low-coercivity minerals, such as magnetite and pyrrhotite, are unlikely to be responsible for the VRM, although they may contribute to the NRM. Hematite seems the most likely carrier of the VRM. Perhaps the VRM contribution increases with depth, as the hematite grows with burial from superparamagnetic to single-domain grain size.

PHYSICAL PROPERTIES

Measurements of compressional-wave velocity, wet-bulk density, porosity, water content, and shear strength

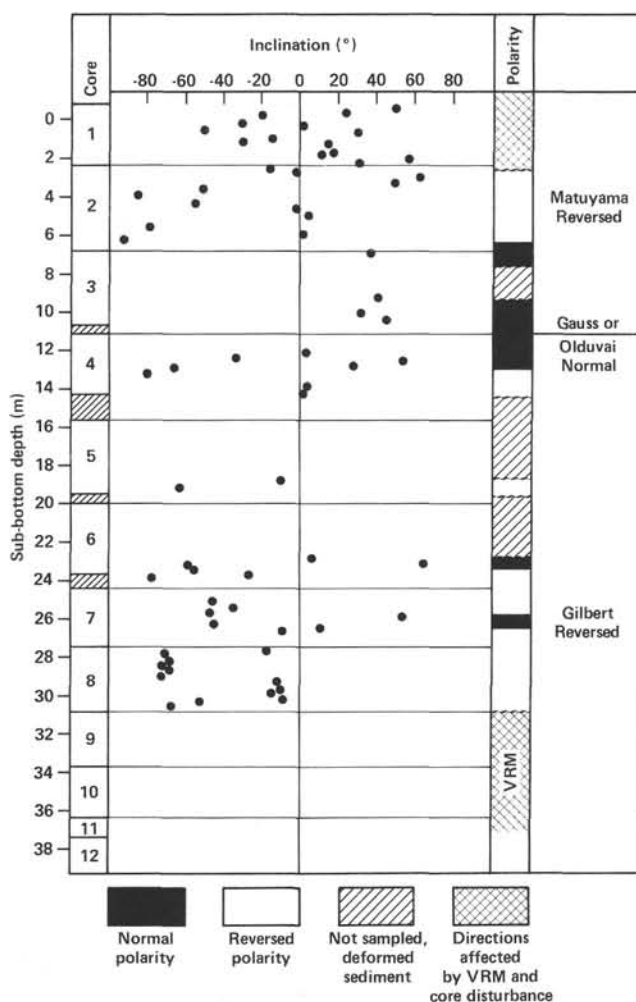


Figure 14. Magnetization versus depth for samples from Hole 544B.

were made at Site 544. The physical properties measured at Hole 544A are summarized in Tables 6 and 7. Figure 15 shows the variation of velocity, density, porosity, water content, and computed acoustic impedance with depth.

Table 6. Physical properties, Site 544.

Core-Section (interval in cm)	Sub-bottom depth (m)	Velocity		GRAPE		Density (g/cm ³)	Porosity (%)	Density (g/cm ³)	Porosity (%)	Water content (%)	Acoustic impedance (10 ⁵ g·cm ⁻² s ⁻¹)
		Horizontal (km/s)	Vertical (km/s)	Density (g/cm ³)	Porosity (%)						
Hole 544A											
1-1, 138-143	1.4	1.54		1.70	59.6	1.67	62.8	37.7			2.57 ^a
1-4, 121-125	5.7	1.52		1.79	54.1	1.73	59.5	34.4			2.64 ^a
2-2, 113-117	9.7	1.54		1.83	51.9	1.75	57.7	32.9			2.69 ^a
2-5, 89-93	13.9	1.55		1.84	51.4	1.78	56.2	31.6			2.76 ^a
3-1, 101-105	17.5	1.56		1.79	54.4	1.75	56.7	32.4			2.72 ^a
4-1, 112-115	27.1	1.56		1.82	52.3	1.81	53.6	29.6			2.82 ^a
5-2, 83-86	37.5	1.55		1.74	57.4	1.81	53.6	29.6			2.80 ^a
6-4, 62-67	50.2	1.55				1.85	51.2	27.7			2.87 ^a
6-4, 67-70	50.2			1.87	49.6						
7-2, 115-117	57.2					1.84	50.7	27.5			
7-2, 117-124	57.2	1.55		1.94	45.3						
8-4, 8-13	68.6			2.09	36.6	1.83	52.2	28.6			
8-4, 15-17	68.7	1.57									
9-4, 44-49	78.5	1.59		1.91	46.9	1.80	54.1	30.1			2.86 ^a
10-5, 108-113	90.1	1.58		1.86	50.4	1.85	52.1	28.2			2.92 ^a
12-1, 25-30	102.3	1.55		1.81	53.4	1.79	54.7	30.6			2.77 ^a
13-1, 36-41	107.9	4.20	3.96	2.62	5.2	2.60	6.1	2.3			10.30
13-1, 80-84	108.3			2.48	13.4						
13-2, 17-22	109.2			2.63	4.3						
14-1, 50-54	112.0	5.65	5.55	2.67	1.7						
15-1, 42-45	121.4					2.57	8.4	3.2			
15-1, 45-48	121.5	4.66	4.40	2.59	7.0						
15-3, 127-130	125.3	5.25	5.06	2.67	2.1						
15-3, 130-133	125.3					2.66	3.0	1.1			
16-1, 23-25	130.2	5.50	5.38	2.68	1.6						
16-1, 26-28	130.3					2.65	3.7	1.4			
19-1, 20-23	149.7	1.75	1.74	2.14	33.7	2.11	38.7	18.3			3.67
20-1, 61-64	157.6	1.79	1.80	2.15	33.2	2.13	36.0	16.9			3.84
20-3, 50-53	160.5	1.67	1.67	2.11	35.3	2.07	40.6	19.6			3.46
21-2, 38-41	167.9	1.80	1.78	2.19	30.5	2.14	36.3	17.0			3.81
26-1, 22-25	206.7	5.74	5.70	2.61	5.5	2.64	1.5	0.6			15.05
27-1, 40-41	216.4			2.62	4.9						
28-1, 23-24	225.7			2.52	11.0						
Hole 544B											
1-1, 68-70	0.7	1.55									
1-1, 131-133	1.3	1.55				1.67	61.4	36.7			2.59 ^a
1-2, 48-50	2.0	1.55									
1-2, 122-124	2.7	1.51		1.69	60.2	1.71	58.9	34.6			2.58 ^a
2-1, 84-86	3.3	1.58				1.75	56.8	32.4			2.76 ^a
2-2, 74-76	4.7	1.56		1.80	53.9	1.73	58.1	33.6			2.69 ^a
2-3, 45-47	5.9	1.55				1.76	56.3	32.0			2.72 ^a
3-1, 121-123	8.0	1.59									
3-3, 44-46	10.3	1.52				1.70	59.5	34.9			2.59 ^a
4-1, 94-96	12.2					1.78	54.9	30.8			
4-1, 146-148	12.7	1.56									
4-2, 121-123	13.9			1.90	47.7						
4-2, 123-125	13.9					1.80	53.2	29.5			
5-1, 70-72	16.3					1.79	53.9	30.1			
5-1, 89-91	16.5	1.56									
5-3, 66-72	19.3	1.54		1.83	52.2	1.75	56.4	32.2			2.69 ^a
6-1, 92-94	20.9					1.79	54.7	30.6			
6-3, 25-27	23.3	1.55									
6-3, 92-94	23.9					1.86	50.6	27.2			
6-3, 134-136	24.4	1.54									
7-1, 100-102	25.4					1.79	54.6	30.5			
8-1, 40-42	27.8					1.83	51.6	28.2			
8-1, 60-64	28.0	1.58		1.87	49.7						
8-3, 10-12	30.5					1.80	53.6	29.8			
8-3, 23-25	30.6	1.56									
9-1, 70-72	31.6					1.83	51.9	28.4			
9-1, 98-100	31.9	1.55									
9-2, 91-93	33.3	1.56									
10-1, 80-82	34.5					1.81	53.2	29.4			
10-1, 121-123	34.9	1.55									
10-2, 60-63	35.8			1.81	53.2						
11-1, 50-52	36.9					1.85	50.6	27.4			
12-1, 20-22	37.6					1.85	50.9	27.5			
12-1, 43-45	37.8			1.81	53.0						
12-2, 8-10	39.0	1.55									

^a Value computed using horizontal velocity.

The variations of the physical properties correlate very well with the observed lithology changes at this site.

Units I (0–102.0 m) and II (102.0–103.8 m) are dominantly clayey foraminiferal–nannofossil oozes. These units are characterized by nearly uniform velocities near 1.55 km/s. Density increases from 1.67 to 1.85 g/cm³, and porosity decreases from 63 to about 53% near the base of Unit II. With the exception of one subsample, GRAPE densities are slightly higher and GRAPE porosities are slightly lower than the corresponding gravimetric densi-

ties and porosities. The shear strength of the ooze generally increases with depth throughout the unit (Table 7). The scatter in the data may be because measurements were made on samples disturbed by drilling. This suggests that the properties measured in these soft sediments may not be representative of *in situ* values.

Unit III (103.8–139.2 m) is a pale reddish brown limestone characterized by measured vertical velocities between 3.96 and 5.55 km/s. Horizontal velocities are 0.10 to 0.26 km/s higher than the vertical velocities. Densi-

Table 7. Shear strength of sediments, Site 544.

Sample (interval in cm)	Sub-bottom depth (m)	Shear strength (kPa)
Hole 544A		
1-1, 80-82	0.8	2
1-4, 114-116	5.7	3
2-5, 70-72	13.7	14
3-1, 93-95	17.4	12
4-1, 102-104	27.0	15
5-2, 79-81	37.5	22
6-4, 59-61	50.1	13
7-2, 126-128	57.3	47
8-4, 17-19	68.7	25
9-4, 40-42	78.4	38
10-5, 116-118	90.2	81
12-1, 23-25	102.2	77
12-1, 112-114	103.1	91
Hole 544B		
1-2, 72-74	2.2	33
2-1, 80-82	3.2	20
2-2, 70-72	4.6	24
2-3, 43-45	5.8	42
3-3, 50-52	10.3	35
4-1, 90-92	12.1	17
4-2, 118-120	13.9	37
5-1, 84-86	16.5	15
5-3, 63-65	19.2	43
6-3, 131-133	24.3	38
7-1, 105-107	25.5	39
7-2, 122-124	27.1	43
8-1, 55-57	28.0	80
8-3, 20-22	30.6	69
9-1, 80-82	31.7	67
9-2, 77-79	33.2	46
10-1, 117-119	34.9	41
10-2, 64-66	35.9	43
11-1, 26-28	36.7	47
12-2, 11-13	39.0	32

ties range from 2.48 to 1.67 g/cm³, and porosities are correspondingly low.

Unit IV (139.2-184.3 m) consists dominantly of reddish brown calcareous and variably sandy muds and friable muddy sands. In this unit, velocities are approximately 1.75 km/s, densities are near 2.15 g/cm³, and porosities are about 33%.

Three physical property samples were taken from the gneiss of Unit V (More than 184.3 m). The velocity is near 5.7 km/s and the density is near 2.64 g/cm³. In order to calculate GRAPE porosities a grain density of 2.65 was assumed for this unit.

The physical properties measured on sediments recovered at the hydraulic piston cored Hole 544B are summarized in Tables 6 and 7. Figure 16 shows the variation of these properties with depth.

The one lithologic unit recognized in this hole is compositionally identical to Unit I in Hole 544A, and the physical properties are nearly identical, except for the shear strength, which is considerably higher at Hole 544B. This may be because the sediments in the two holes are disturbed to different degrees.

SEISMIC STRATIGRAPHY

During the approach to Site 544, the satellite navigation system failed. The approach was based on the Omega, navigation system, celestial navigation, and echo sounding, using a bathymetric chart prepared for Leg 79 and multichannel seismic data. Seismic, magnetic, and bathymetric measurements were made during the entire track from Las Palmas to Site 544. The seismic measurements were made with the *Glomar Challenger* system, consisting of a single-channel analog recording unit, a Teledyne streamer, and two Bolt air guns (120 and 40 cu. in.).

Site 544 is located on the northwestern flank of a north-northwest/south-southeast trending terracelike feature, about 150 km², at 3200 to 3900 m water depth (Fig. 17), which adjoins the Mazagan Plateau to the west.

The seismic coverage near Site 544 (Fig. 18) includes multichannel seismic lines (*Meteor* M 53-01 to M 53-10, *Meteor* M 39-01, *Valdivia* 79-02/04/05) and single-channel lines (*Vema* cruise VE 3013, *Glomar Challenger* Leg 41). Holes 544, 544A, and 544B are located about 500 m southeast of line M 53-08, at the side wall of a steeply (15-30°) sloping escarpment approximately 500 m high. Figure 19 shows part of seismic line M 53-08, on which the interpreted seismic sequence and seismic markers are indicated. The nature of the structure beneath Site 544 has been a subject of discussion because granitic fragments were found in piston-cored samples from *Vema* cruise VE 3013 and in dredge samples retrieved from the escarpment during *Valdivia* West Africa cruise 1979. The structure has been variously interpreted: as slivers of foundered continental basement, pushed upward along landward-dipping thrust faults; as an autochthonous basement ridge (Wissmann and von Rad, 1979); and as a salt structure, owing to its similarity in size and structural seismic pattern to numerous piercing structures shown on seismic profiles off Morocco and interpreted as salt domes.

Correlation of Seismic Data with Drilling Results

At Site 544 there is only one seismic marker, the Blue reflector (Horizon B in Fig. 20), which represents the top of Sequence Ma 3, interpreted as consisting of Jurassic carbonates. (For a general description of seismic sequences in the Mazagan region, see the regional synthesis chapter by Winterer and Hinz, this volume.)

The Red reflector (Horizon R in Fig. 20), which forms the lower boundary of the Neogene Sequences Ma 1.1, Ma 1.2 and Ma 1.3, terminates with onlap against the Blue reflector a little east of Site 544 (Fig. 20). The younger unconformity, tentatively assigned a Neogene age, also pinches out against the Blue reflector. The Blue reflector forms the upper boundary of a sequence approximately 0.5 s thick, characterized by a discontinuous reflection pattern. The same relations hold for line M 53-10, located about 450 m north of the holes, and for the *Glomar Challenger* single-channel line recorded during the approach to Site 544.

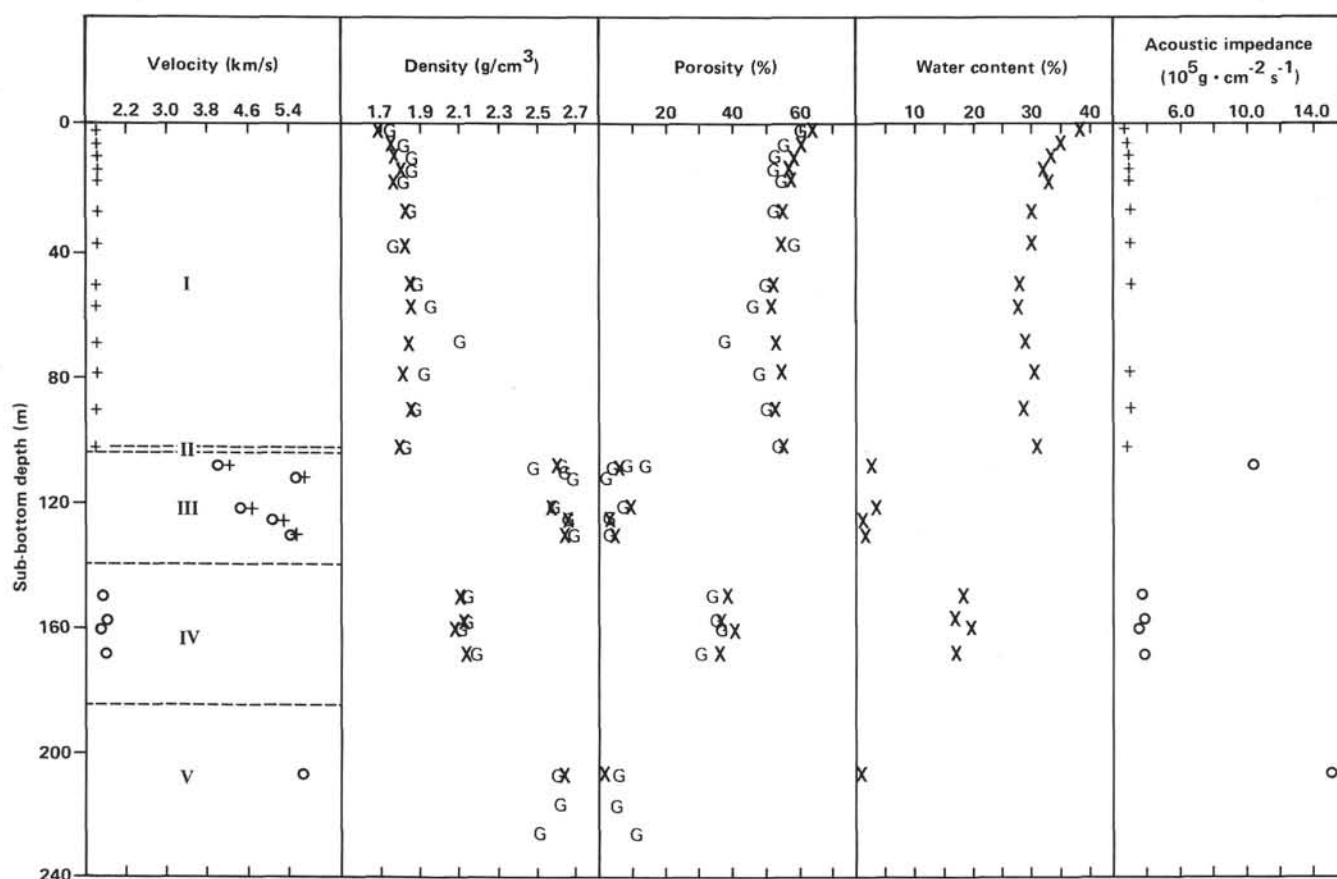


Figure 15. Physical properties versus depth, Hole 544A. +, O represent horizontal and vertical values, respectively. X, G represent gravimetric (immersion) and GRAPE values, respectively.

On line *M* 53-10 (Fig. 21), the Blue reflector lies 0.135 s (two-way reflection time) beneath the seafloor at the projected Site 544 and correlates well with the top of Lithologic Unit III, which consists of reddish brown limestone encountered 103.8 m beneath the seafloor. This correlation implies an average interval velocity of about 1540 m/s for the Cenozoic interval (Pliocene-Pleistocene and Miocene; Cores 544A-1-12).

The reflector at 4.97 s (reflection time) which lies 0.05 s beneath the Blue reflector at the projected site location on line *M* 53-10 (Fig. 21) very probably correlates with the top of the drilled gneiss of Unit V, 184 m beneath the seafloor (see also Fig. 22). Such a correlation implies an average interval velocity of 3200 m/s for Units III and IV, lying between the top of the Jurassic limestone and the top of the gneiss (Cores 12-22). The Jurassic limestone beds are apparently too thin to become seismically resolvable because both top and bottom reflections are within about one wavelet.

Table 8 shows the reflection times to the major reflectors identified on seismic reflection profiles passing close to Site 544, and the interval velocities deduced for the major lithologic units drilled at Site 544.

SUMMARY AND CONCLUSIONS

Site 544 was drilled on a structurally high block from which fragments of granitic rock had been cored and

dredged, in the vicinity of rather similar high blocks which have many characteristics, such as rim synclines, suggesting that they are salt diapirs. The seismic interpretation of the structure at Site 544 is ambiguous: it shows upwardbending of sedimentary reflectors in the adjacent basins that might be the result of diapiric intrusion, of drag along faults, or simply of compactional folding over a rigid block. The dredged fragments of granitic rock might have been dragged upward along the edge of a diapir, or they might be in place. Because acoustic basement appears actually to crop out along the escarpment a few hundred meters northwest of the site, the risk of finding an accumulation of hydrocarbons at Site 544 is very low. Thus, the site was ideal to test whether the acoustic basement in that area is salt or sial.

The result of drilling was to prove the sial hypothesis, but the cores brought back much more than simply that answer. We obtained a relatively condensed record, 104 m thick, of Neogene pelagic sedimentation that includes at least two hiatuses in the Miocene, and then an extraordinarily well preserved section, about 35 m thick, of reddish Jurassic limestone strikingly similar to the red oncoloidal and skeletal limestone of Oxfordian age dredged from the Mazagan Escarpment (Renz et al., 1976). Beneath the limestone we encountered about 45 m of reddish sandy mudstone and gneissic gravel, probably non-

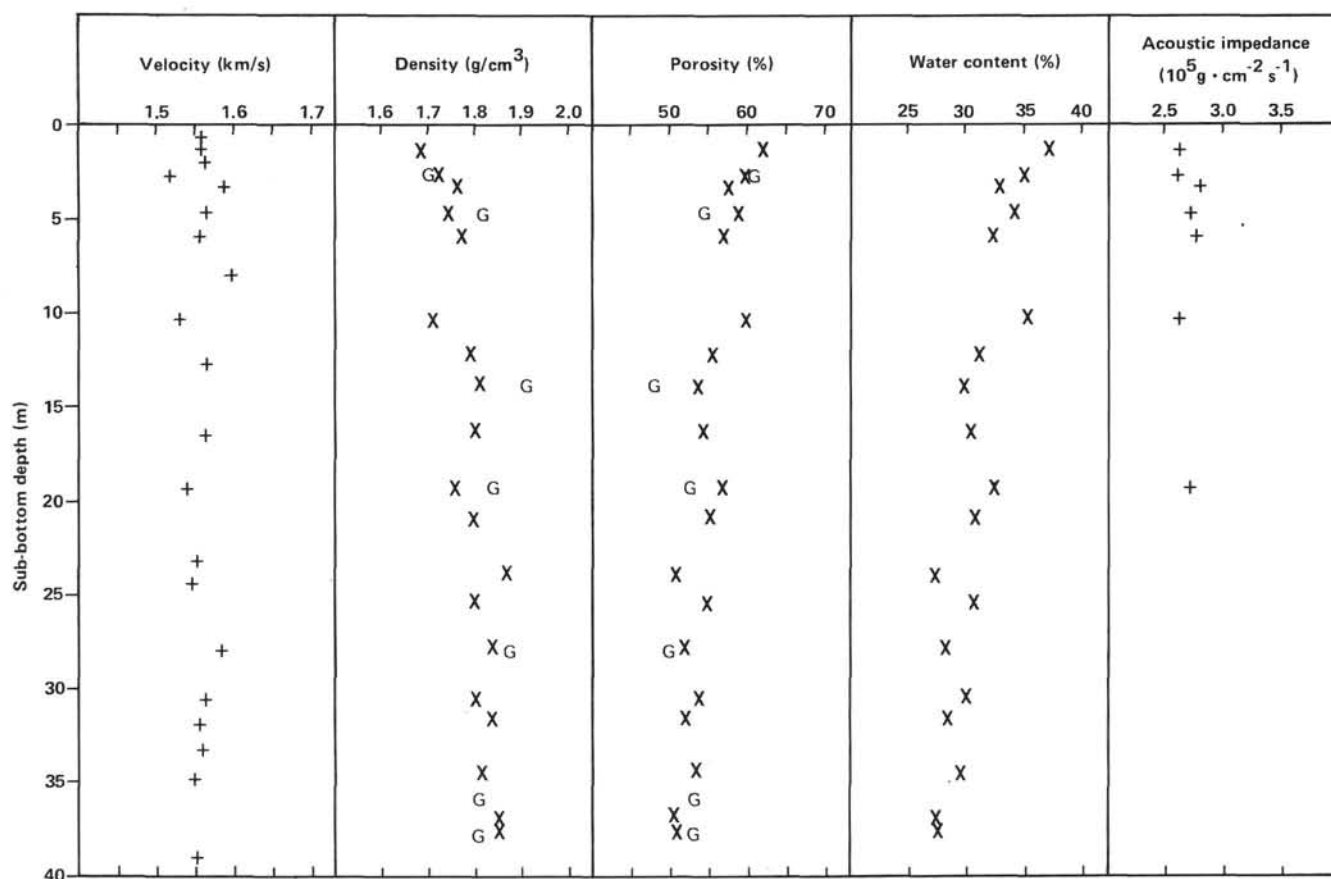


Figure 16. Physical properties versus depth, Hole 544B. +, × represent horizontal and vertical values, respectively. ×, G represent gravimetric (immersion) and GRAPE values, respectively.

marine in origin, resting directly on a basement of granitic gneiss. The drilling results are summarized graphically in Figure 2, and in more detail in Figure 23.

Neogene Sediments

The Neogene section is truncated at the top because we chose the drill site at a place where erosion near the escarpment exposes the youngest acoustic reflectors. We tried to choose a spot where there was just enough soft sediment to bury the bottom-hole assembly; in fact, we spudded in ooze of early Pleistocene age, and at depth of only 11 m microfossils of Pliocene age were identified. The seismic profiler records suggest that close by the site another 50 m or so of Pleistocene sediment lies above the stratigraphic level where we spudded.

With the caveat that the spacing of shipboard paleontological samples may be too coarse to detect minor unconformities, we believe that the lowest Pleistocene to upper Miocene section appears continuous down to about 56 m depth. There is a discrepancy between foraminiferal and nannofossil age assignments close to the Pliocene/Miocene boundary that will have to be resolved by postcruise studies. A glauconitic zone at a depth of about 56 m separates late Miocene fossils of Zone N17 from middle Miocene fossils of Zone N14. Sediments above the hiatus are mainly well-oxidized foraminiferal and nannofossil ooze. Both carbonate content and the pro-

portion of foraminifers decrease downward toward the hiatus.

The hiatus represents about 4 m.y. of missing record, and the section skips from some place near the base of the Messinian Stage to some place in the upper part of the Serravallian; the Tortonian is absent, or represented only in highly condensed form. The unconformity at this place in the column may be quite local; no such hiatus is recorded at Site 370 (416) in the nearby Morocco Basin (Vincent et al., 1980). On the other hand, at two other (perhaps three) sites on the continental slopes of Northwest Africa—Site 397 off Cape Bojador (Salvatorini and Cita, 1979), Site 367 on the Sierra Leone Rise, and perhaps Site 369 off Cape Bojador (Lancelot, Seibold, et al., 1978)—a hiatus separates foraminiferal Zones N16 and N14 (lower Tortonian and upper Serravallian). Perhaps deep thermohaline boundary currents eroded and winnowed sediments on the slopes.

The upper 39.3 m of the Neogene section were resampled with the hydraulic piston corer in Hole 544B. The sediments were far less disturbed than in the conventional cores, but showed nothing unexpected. The HPC extended nearly its full 4.5 m in the first few cores, but began to decrease its stroke to less than 4 m at 7 m depth, to less than 3 m at 31 m depth, and to less than 2 m at 36 m. The measured vane shear strength of the deepest HPC cores was only about 40 kPa, a value far

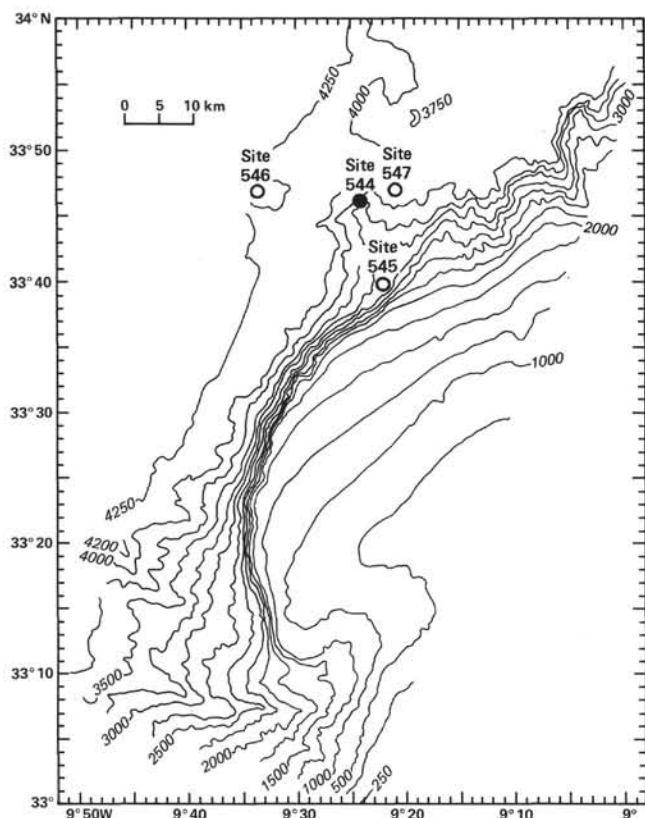


Figure 17. Bathymetric map of the Mazagan continental margin segment, from echo soundings of *Meteor* cruises 9/1967, 39/1975, 53/1980, the *Valdivia* West Africa cruise 1979, and the SEAZAGAN seabeam survey of *Jean Charcot* (Auzende et al., this volume). Depths in m.

less than the limiting strength for HPC cores in pelagic ooze. Probably the behavior of the HPC in Hole 544B is related to the high clay content of the sediments, which ranged from about 30 to 45%.

The chief motive for obtaining HPC cores at Site 544 was to sample for paleomagnetic reversals, but the results were disappointing. Several cores were disturbed because the core liner cracked during coring, and all cores have a viscous remanent magnetization that was probably acquired, very rapidly, after coring. The original magnetic signal of many samples is thus spoiled, and we have scant hope of documenting a good polarity reversal sequence.

Beneath the unconformity, the lowest middle Miocene sediments are more greenish, and pyrite, glauconite, and Fe-Mn are recorded at many levels in cores near the upper boundary. These sediments consist of foraminiferal-nannofossil and nannofossil ooze, which is firmer downward and is as hard as chalk near the base of this unit, at a depth of 102.6 m.

At 102.6 m, beds with fossils of the very late early Miocene (N9) overlie strata with somewhat older early Miocene fossils (N7). There may be a small hiatus here: the sediments are glauconitic nannofossil chalk and nannofossil-bearing claystone.

Only 2 m lower, at 103.8 m, the Neogene pelagic sediments rest directly on Jurassic limestone, and this unconformity thus gathers up and blends all the hiatuses

between. We are simply unable to say from the evidence at hand at Site 544 whether this represents a very long period of nondeposition, or whether post-Oxfordian(?) sediments were at one time deposited here and subsequently eroded. The major regional hiatus that effectively eliminates most of the Upper Cretaceous (Lancelot and Winterer, 1980) and the well-known episode of extensive erosion of deep sea and continental margin sediments during the Oligocene may both be hidden in the gap at Site 544.

As to the Neogene environmental conditions recorded at Site 544, the good preservation of foraminifers over most of the column attests to a position above the foraminiferal lysocline. At the same time, the net sedimentation rate of about 7 m/m.y. in the late Miocene to early Pleistocene is rather slow for calcareous oozes in a relatively fertile region above the lysocline; it suggests either that currents may have winnowed out something like half the sediment that fell here during that time, or that there may be undetected diastems. The rate estimated for the early and middle Miocene is about 8 m/m.y., and the common glauconite in the middle Miocene suggests slow rates. Perhaps small hiatuses punctuate this part of the record.

Mesozoic Rocks

At 103.8 m the drill entered red Jurassic limestone, consisting mainly of skeletal particles and intraclasts packed together with a micritic matrix. Some patches have a sparry calcite cement rather than a micrite matrix, and in some the grains do not form a rigid framework but are supported by the lime mud. The intraclasts are mainly bioclasts enveloped in micrite coatings. Oncoids are common at some levels, and some are encrusted by miliolids.

The skeletal components are both pelagic and benthic. Pelagic *Bositra* ("Posidonia"), *Protoglobigerina*, and small ammonites occur together with echinoids, crinoids, ostracodes, small gastropods, vagile foraminifers (miliolids, nodosariids), terebratulide, brachiopods, bivalves, sponge fragments, serpulid worm tubes, bryozoans, and a solitary coral. In many places shells and crinoid columnals are still articulated, but most shells show the effects of microborings, perhaps by endolithic algae. The "churned" fabric of the limestone indicates extensive bioturbation.

Hardgrounds are numerous and show good evidence of lithification and encrustation by Fe-Mn and then by serpulids and foraminifers. Cavities floored by internal sediment and filled with sparry calcite are common.

The cement in the grainstones shows a first phase of radialial calcite, suggesting seawater as the milieu.

The combination of textural and biological features in this limestone suggests a diverse benthos supported by algal or cyanobacterial activity, on a firm substrate where currents were occasionally strong enough to rework and sort grains. The net rate of accumulation was probably low and at times was effectively zero. The red color indicates thorough oxidation of all organic matter.

Site 544 is on a horst of crystalline basement, and it is possible that this was so even in Jurassic times; that is, the limestone may have been deposited on a topographic

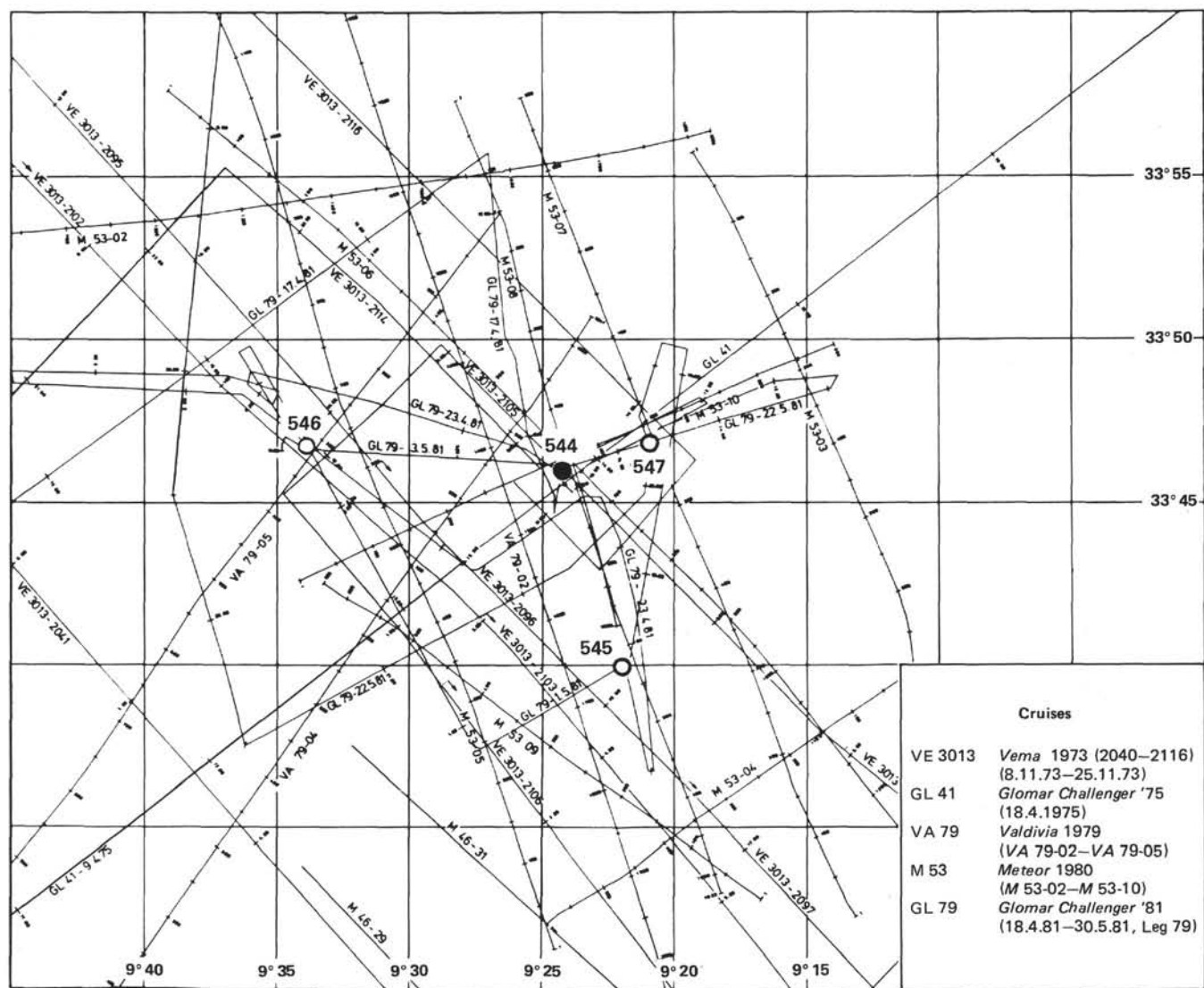


Figure 18. Location of seismic profiles around Site 544.

ridge that was protected from clastics spreading seaward from the shoreline to the southeast by a deeper water trough. Renz et al. (1975), however, describe very similar red limestone dredged from outcrops 20 km to the southeast on the Mazagan Escarpment.

The high values of sound velocity measured in the red limestone render certain the identification of acoustic basement with the top of the limestone.

At about 139 m, the red limestone gives way downward to red sandy mudstone. The nature of the contact and even its location are very uncertain owing to very poor core recovery in the interval from 130 to 150 m; there may even be a whole transitional facies missing from the cores. The muddy strata between 139 m and the top of the gneissic basement are at least 35 and more likely 45 m thick. The upper 30 m, down to about 168 m, are mainly sandy mudstone and muddy sandstone and show many examples of slump folds and soft sediment deformation. In the lowest few meters, just above basement, the core recovered angular gneissic pebbles.

We interpret this sequence, in which no fossils could be found, as terrestrial, in origin. There was doubtless some local relief on the original gneissic terrane, and alluvial deposits accumulated on and at the base of local slopes, gradually decreasing in caliber as relief was buried. Gradients were steep enough to permit mud flows, and the climate was doubtless warm and probably seasonally dry. Erosion rates were rapid and very fresh feldspar was transported and buried before alteration. Whether the red color developed *in situ* or is mainly derived from upland soils is not clear.

Basement Rocks

The crystalline basement is gneissic and granitic in composition. The cataclastic texture is distinctive, and this should make easier a search for possible analogs in the basement rocks on the Moroccan Meseta. The foliation is subhorizontal. The gneiss is stained pink, even at a depth of 50 m below the covering red sediments, and

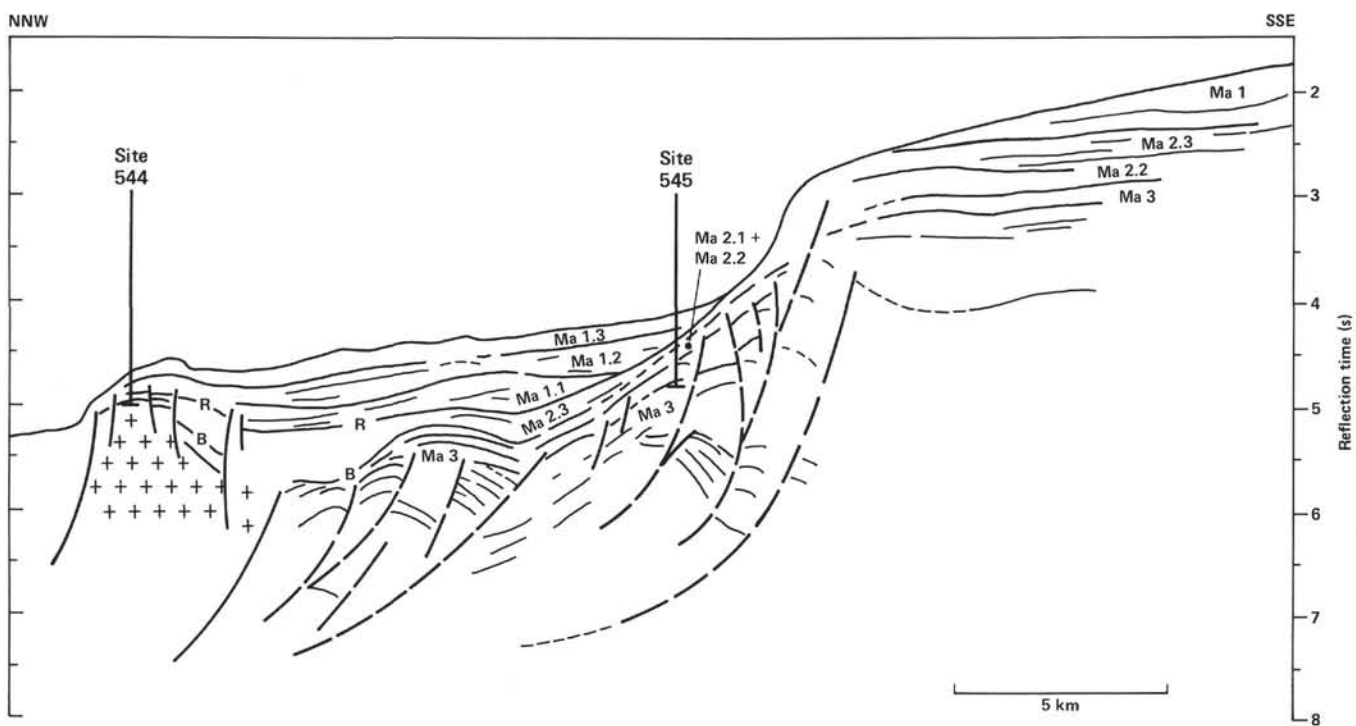
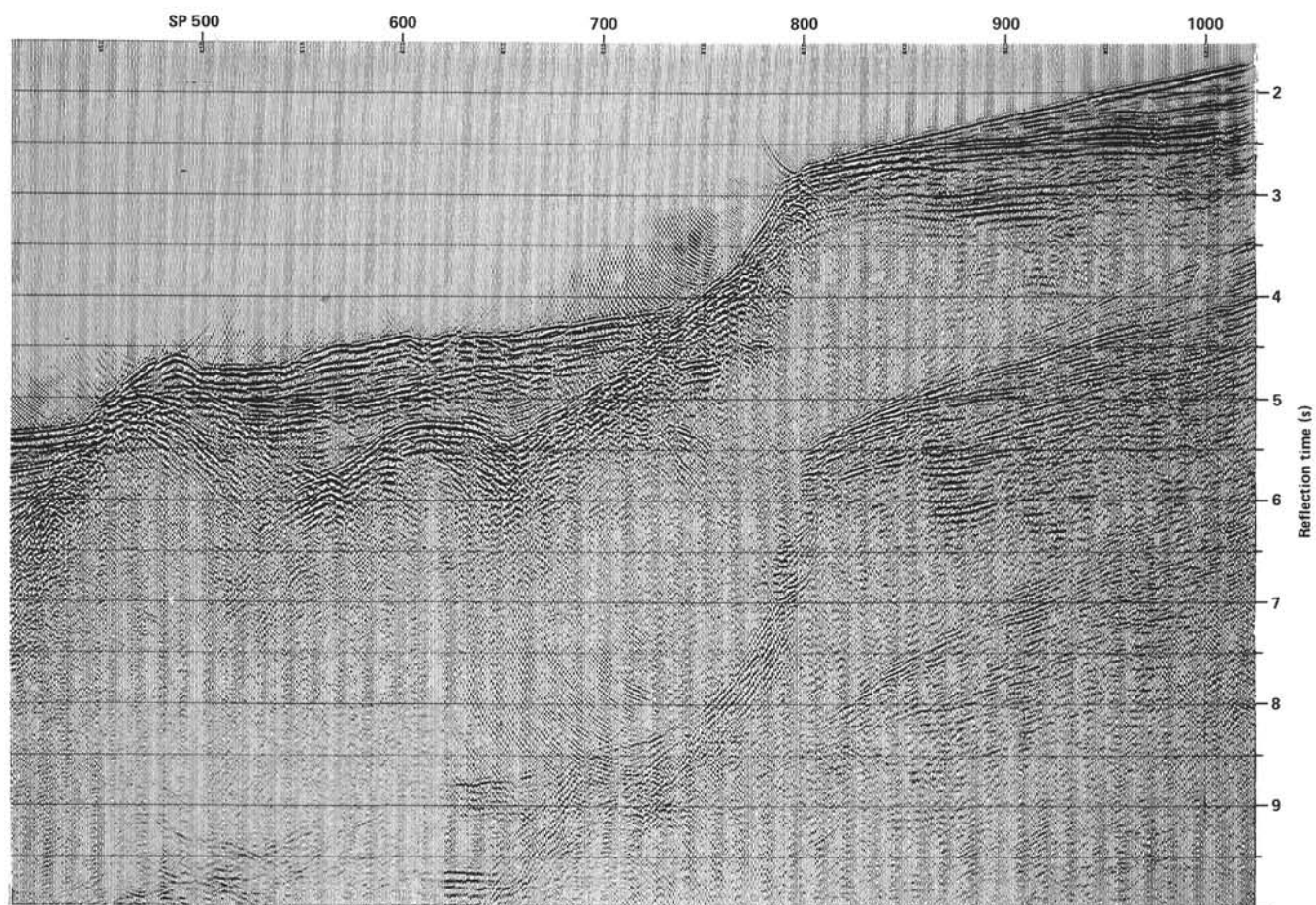


Figure 19. Seismic record of *Meteor* line *M* 53-08 and line drawing with reflectors and identified seismic sequences near Site 544. Location of the profile is indicated in Figure 18. See text for discussion of features.

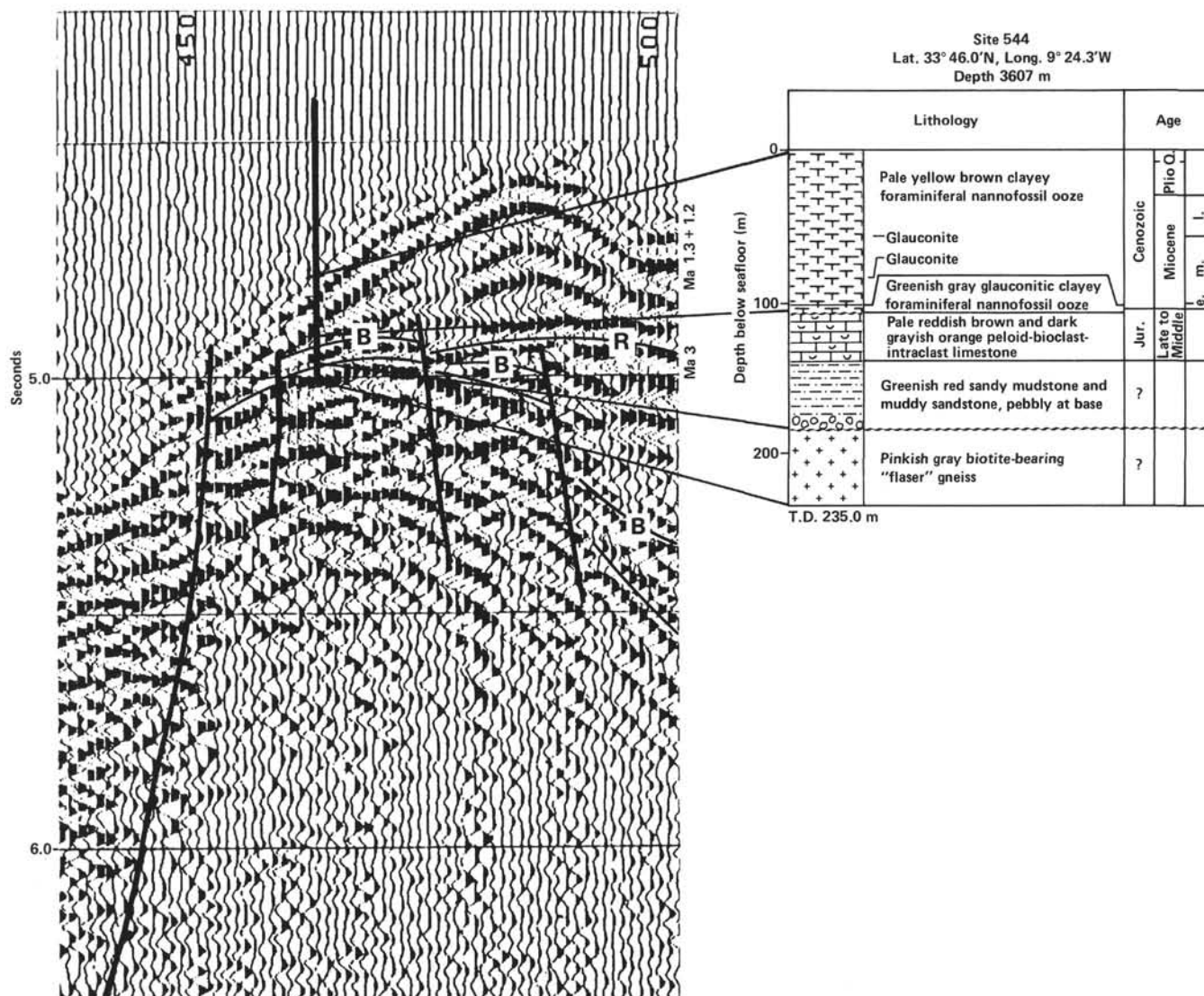


Figure 20. Correlation of reflectors and seismic sequences from seismic reflection profile M 53-08 with the drilling results of Site 544. B, blue reflector; R, red reflector.

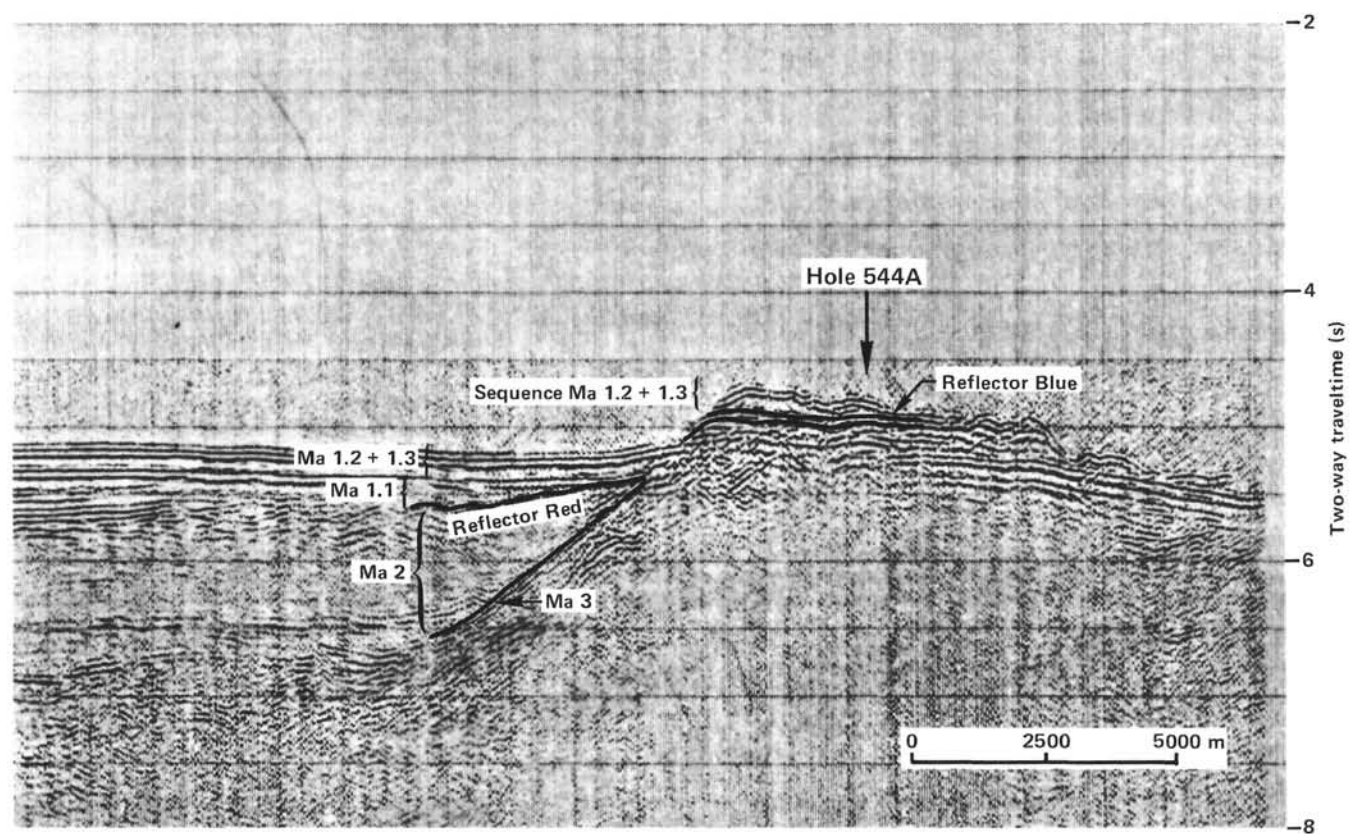


Figure 21. Seismic record of *Meteor* line M 53-10 and identified seismic sequences near Site 544. Location of the profile is indicated in Figure 18.

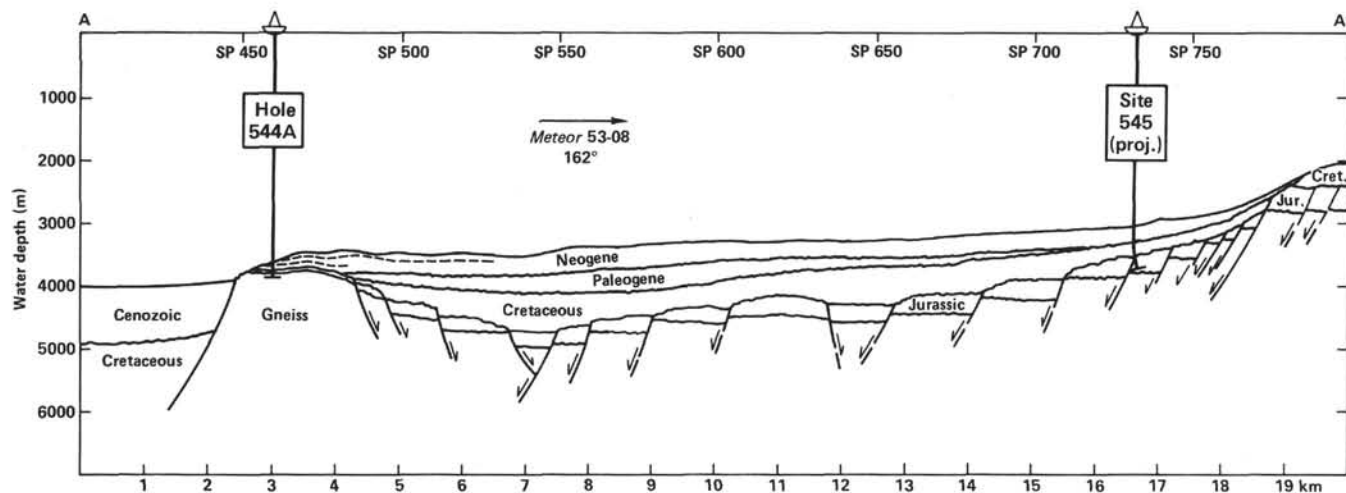


Figure 22. Geologic cross section through Site 544, along *Meteor* seismic line *M* 53-08 (line A-A' on Figure 4).

Table 8. Two-way reflection times from sea surface to key reflectors and interval velocities between reflectors identified at Site 544.

Seismic sequences and markers	Reflection time (s)			Sub-bottom depth (m)	Interval velocity (km/s)					
	Line <i>M</i> 53-10 A	Line <i>M</i> 53-08 B	Line <i>GC</i> 41 C'		A	B	C'	A	B	C
Seafloor	4.745	4.78	4.77							
Ma 1.1 + 1.2					1.54	1.60	1.49			
Blue	4.88	4.91	4.91	104				1.54	1.60	1.49
Ma 3					3.20	3.20		1.99		2.04
Top of gneiss	4.93	4.96		184						

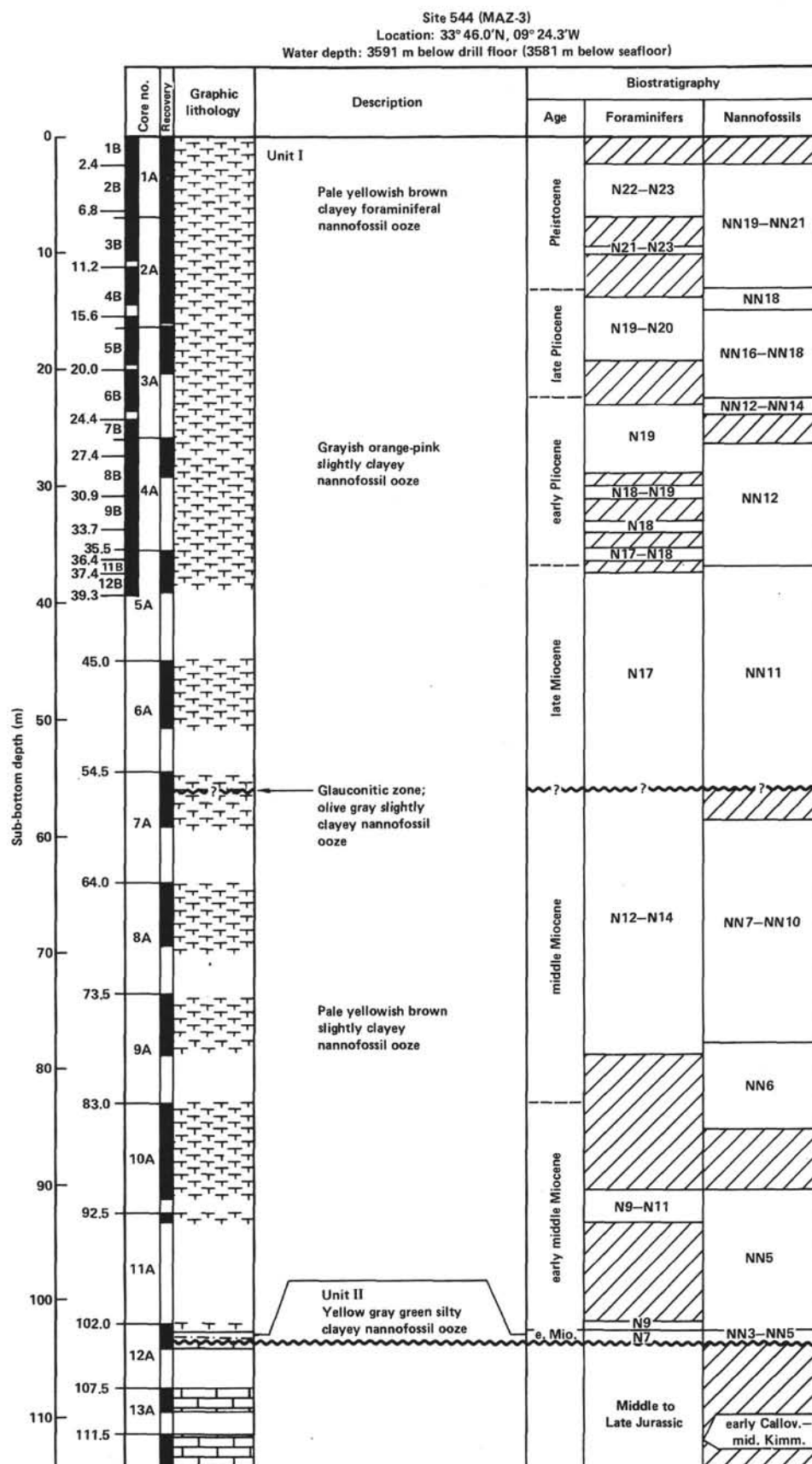


Figure 23. Detailed graphic log of Site 544 (Holes 544A and 544B).

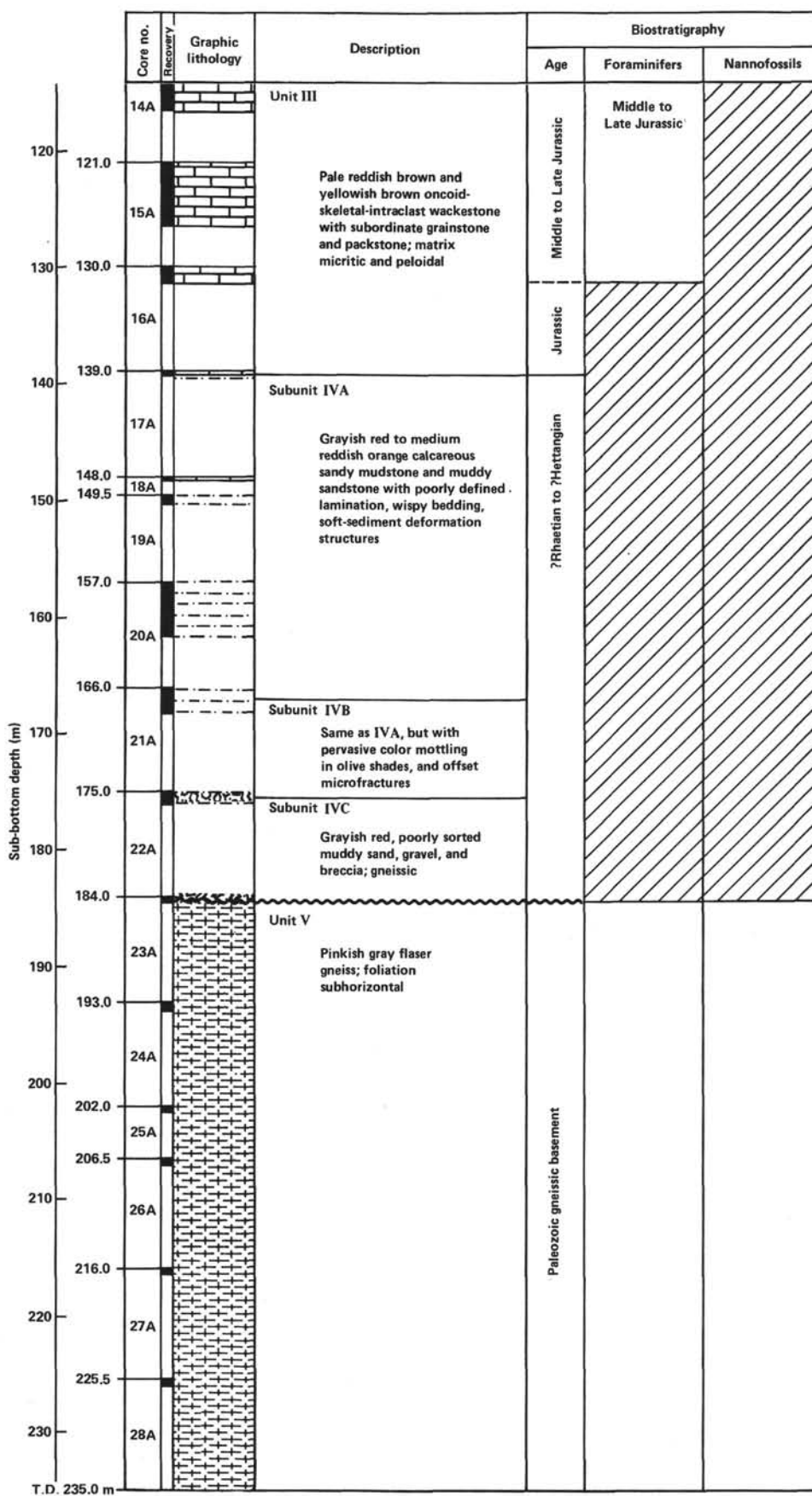


Figure 23. (Continued).

SITE	544	HOLE	A	CORE	2	CORED INTERVAL	7.0-16.5 m sub-bottom																																																																																																																													
TIME - ROCK UNIT	BIOSTRATIGRAPHIC ZONE	FOSSIL CHARACTER		SECTION	METERS	GRAPHIC LITHOLOGY	LITHOLOGIC DESCRIPTION																																																																																																																													
		FORAMINIFERS	NANNOFOSSILS																																																																																																																																	
		RADOLARIAE	DIAZOME																																																																																																																																	
						DRILLING DISTURBANCE DISTURBANCE STRUCTURAL SAMPLES																																																																																																																														
late Pliocene to Pleistocene	N21-22 (F) Discoaster brownii zone (N)	AG	CG		0.5	Void																																																																																																																														
				1	1.0																																																																																																																															
				2																																																																																																																																
				3																																																																																																																																
				4																																																																																																																																
				5																																																																																																																																
				6																																																																																																																																
				CC																																																																																																																																
<p>Moderately to highly disturbed, greyish orange-pink (5YR 7/2) to pale yellowish brown (10YR 6/2) VERY CLAYEY NANNOFOSSIL FORAMINIFERAL OOZE.</p> <p>Massive 50-60 cm thick layers of either color alternate with interbedded 1-2 cm thick layers of both colors. Locally in Section 3, common in Section 4, black FeS/Mn? mottling or burrow-fills, and associated darker layers.</p> <p>SMEAR SLIDE SUMMARY (%):</p> <table><tr><th></th><th>1, 120</th><th>2, 70</th><th>2, 130</th><th>3, 120</th><th>4, 100</th></tr><tr><th></th><th>D</th><th>O</th><th>D</th><th>D</th><th>D</th></tr><tr><td>Texture:</td><td></td><td></td><td></td><td></td><td></td></tr><tr><td>Sand</td><td>15</td><td>10</td><td>20</td><td>30</td><td>25</td></tr><tr><td>Silt</td><td>10</td><td>10</td><td>10</td><td>10</td><td>20</td></tr><tr><td>Clay</td><td>75</td><td>80</td><td>70</td><td>60</td><td>55</td></tr><tr><td>Composition:</td><td></td><td></td><td></td><td></td><td></td></tr><tr><td>Quartz</td><td>Tr</td><td>Tr</td><td>Tr</td><td>5</td><td>5</td></tr><tr><td>Feldspar</td><td>-</td><td>-</td><td>-</td><td>-</td><td>2</td></tr><tr><td>Clay</td><td>5</td><td>5</td><td>10</td><td>15</td><td>16</td></tr><tr><td>Iron oxide</td><td>Tr</td><td>Tr</td><td>-</td><td>Tr</td><td>-</td></tr><tr><td>Glauconite</td><td>-</td><td>-</td><td>-</td><td>Tr</td><td>-</td></tr><tr><td>Pyrite</td><td>-</td><td>-</td><td>-</td><td>-</td><td>1</td></tr><tr><td>Amphibol</td><td>-</td><td>-</td><td>-</td><td>Tr</td><td>-</td></tr><tr><td>Foraminifers</td><td>10</td><td>10</td><td>15</td><td>25</td><td>30</td></tr><tr><td>Calc. nannofossils</td><td>80</td><td>80</td><td>70</td><td>50</td><td>45</td></tr><tr><td>Sponge spicules</td><td>-</td><td>-</td><td>Tr</td><td>-</td><td>-</td></tr><tr><td>Fish remains</td><td>Tr</td><td>-</td><td>-</td><td>-</td><td>-</td></tr><tr><td>Dolomite</td><td>-</td><td>Tr</td><td>Tr</td><td>Tr</td><td>Tr</td></tr></table> <p>ORGANIC CARBON AND CARBONATE (%):</p> <table><tr><th></th><th>4, 142-144</th><th>4, 144-150</th></tr><tr><td>Carbonate</td><td>41.5</td><td>54.5</td></tr><tr><td></td><td>5, 118-120</td><td>6, 0-2</td></tr><tr><td>CaCO₃</td><td>57.0</td><td>62.0</td></tr></table>								1, 120	2, 70	2, 130	3, 120	4, 100		D	O	D	D	D	Texture:						Sand	15	10	20	30	25	Silt	10	10	10	10	20	Clay	75	80	70	60	55	Composition:						Quartz	Tr	Tr	Tr	5	5	Feldspar	-	-	-	-	2	Clay	5	5	10	15	16	Iron oxide	Tr	Tr	-	Tr	-	Glauconite	-	-	-	Tr	-	Pyrite	-	-	-	-	1	Amphibol	-	-	-	Tr	-	Foraminifers	10	10	15	25	30	Calc. nannofossils	80	80	70	50	45	Sponge spicules	-	-	Tr	-	-	Fish remains	Tr	-	-	-	-	Dolomite	-	Tr	Tr	Tr	Tr		4, 142-144	4, 144-150	Carbonate	41.5	54.5		5, 118-120	6, 0-2	CaCO ₃	57.0	62.0
	1, 120	2, 70	2, 130	3, 120	4, 100																																																																																																																															
	D	O	D	D	D																																																																																																																															
Texture:																																																																																																																																				
Sand	15	10	20	30	25																																																																																																																															
Silt	10	10	10	10	20																																																																																																																															
Clay	75	80	70	60	55																																																																																																																															
Composition:																																																																																																																																				
Quartz	Tr	Tr	Tr	5	5																																																																																																																															
Feldspar	-	-	-	-	2																																																																																																																															
Clay	5	5	10	15	16																																																																																																																															
Iron oxide	Tr	Tr	-	Tr	-																																																																																																																															
Glauconite	-	-	-	Tr	-																																																																																																																															
Pyrite	-	-	-	-	1																																																																																																																															
Amphibol	-	-	-	Tr	-																																																																																																																															
Foraminifers	10	10	15	25	30																																																																																																																															
Calc. nannofossils	80	80	70	50	45																																																																																																																															
Sponge spicules	-	-	Tr	-	-																																																																																																																															
Fish remains	Tr	-	-	-	-																																																																																																																															
Dolomite	-	Tr	Tr	Tr	Tr																																																																																																																															
	4, 142-144	4, 144-150																																																																																																																																		
Carbonate	41.5	54.5																																																																																																																																		
	5, 118-120	6, 0-2																																																																																																																																		
CaCO ₃	57.0	62.0																																																																																																																																		

SITE	544	HOLE	A	CORE	3	CORED INTERVAL	16.5-26.0 m sub-bottom							
TIME - ROCK UNIT	BIOSTRATIGRAPHIC ZONE	FOSSIL CHARACTER				SECTION	METERS	GRAPHIC LITHOLOGY	DRILL LOG	DEVIANCE	RESISTIVITY	TEMPERATURE	SAMPLES	LITHOLOGIC DESCRIPTION
		FORAMINIFERS	NANNOFOSSILS	RADICULARIANS	DATUMS									

SITE 544		HOLE A		CORE 4		CORED INTERVAL		26.0–35.5 m sub-bottom	
TIME – ROCK UNIT	BIOSTRATIGRAPHIC ZONE	FOSSIL CHARACTER			SECTION METERS	GRAPHIC LITHOLOGY	DRILLING SEQUENCE STRUCTURES	SAMPLES	LITHOLOGIC DESCRIPTION
		FORAMINIFERS	NANNOFOSSILS	RADIOLARIANS					
early to middle Pliocene	<i>Globobulimina marginata</i> zone (N19) (F)				1				Slightly to moderately disturbed, grayish orange-pink (5YR 7/2) with zones of pale pinkish-gray (5YR 8/1) CLAYEY FORAMINIFERAL-NANNOFOSSIL Ooze. Occasional dark gray (N3–N4) Fe/Mn? laminae. XRD: mainly illite, possibly some smectite mixed-layers. SMEAR SLIDE SUMMARY (%): 1, 100 D Texture: Sand 5 Silt 15 Clay 70 Composition: Quartz 2 Feldspar Tr Clay 20 Foraminifers 10 Calc. nannofossils 68 ORGANIC CARBON AND CARBONATE (%): 1, 144–150 2, 78–79 Carbonate 69.1 78.8
		CG	CG		2				

SITE 544		HOLE A		CORE 5		CORED INTERVAL		35.5–45.0 m sub-bottom	
TIME – ROCK UNIT	BIOSTRATIGRAPHIC ZONE	FOSSIL CHARACTER			SECTION METERS	GRAPHIC LITHOLOGY	DRILLING SEQUENCE STRUCTURES	SAMPLES	LITHOLOGIC DESCRIPTION
		FORAMINIFERS	NANNOFOSSILS	RADIOLARIANS					
late Miocene to early Pliocene	<i>G. aculeolosa</i> / <i>G. marginata</i> zone (N17–18) (F) <i>Ceratomyxina</i> <i>primitiva</i> Pliocene (top NN11) (N)				1				Soupy to undisturbed, grayish orange-pink (5YR 7/2) to pale yellowish brown (10YR 6/2) CLAYEY NANNOFOSSIL Ooze. Common color interlayering, with tendency to paler yellowish gray (5Y 7/2), 1–8 cm thick interlayers (Section 2, 14–27 cm) and change to pinkish gray (5YR 8/1) at Section 2, 32 cm. Thin dark gray to black (N4–N2) laminae (FeS?) in Section 1, 148 cm and Section 3, 19 cm. SMEAR SLIDE SUMMARY (%): 1, 120 D Texture: Sand – Silt 15 Clay 85 Composition: Clay 15 Foraminifers 1 Radiolarians Tr Dolomite 3 ORGANIC CARBON AND CARBONATE (%): 2, 28–29 2, 118–120 3, 0–2 Carbonate 69.4 72.6 69.6
		GA	CM	B	2				
					3				

SITE 544		HOLE A		CORE 6		CORED INTERVAL		45.0–54.5 m sub-bottom	
TIME – ROCK UNIT	BIOSTRATIGRAPHIC ZONE	FOSSIL CHARACTER			SECTION METERS	GRAPHIC LITHOLOGY	DRILLING SEQUENCE STRUCTURES	SAMPLES	LITHOLOGIC DESCRIPTION
		FORAMINIFERS	NANNOFOSSILS	RADIOLARIANS					
late Miocene to early Pliocene	<i>Discosphaera quinquevittata</i> zone (NN11) (N)				1				Drilling slurry and few moderately disturbed (base of core) grayish orange-pink (5YR 7/2) to pale yellowish brown (10YR 6/2) CLAYEY NANNOFOSSIL Ooze. Section 4 shows 1 mm to 2 cm thick interlayering of the two colors. Few medium gray (N5) laminae in Section 4. SMEAR SLIDE SUMMARY (%): 1, 120 2, 100 4, 70 D D D Texture: Sand Tr 5 1 Silt 15 5 4 Clay 85 90 95 Composition: Quartz 2 Tr – Feldspar Tr? Tr – Clay 12 10 10 Pyrite – Tr Tr Foraminifers 6 5 1 Calc. nannofossils 80 80 85 Dolomite – Tr Tr ORGANIC CARBON AND CARBONATE (%): 4, 40–41 Carbonate 75.2
		FG	CG	R	2				
					3				
					4				

SITE 544 HOLE A CORE 7 CORED INTERVAL 54.5–64.0 m sub-bottom

TIME – ROCK UNIT	BIOSTRATIGRAPHIC ZONE	FOSSIL CHARACTER			SECTION METERS	GRAPHIC LITHOLOGY	FOSSILS DISTURBANCE SEDIMENTARY STRUCTURES SAMPLES	LITHOLOGIC DESCRIPTION																														
		FORAMINIFERS	NANNOFOSSILS	RADIOLARIANS																																		
late Miocene	N17 (F) NN11 (N)				0.5		* AR	Below 85 cm of drilling slurry, slightly disturbed light olive gray (5Y 6/1), light gray (N7) to brownish gray (5YR 4/1) CLAYEY TO VERY CLAYEY NANNOFOSSIL OOZE. In Section 1, 10–84 cm mixed chunks of pale orange-pink (5YR 7/2) slightly clayey and of light olive gray (5Y 6/1) ooze below that, firmer, finely laminated ooze. In Section 2 abundant dark gray (N3) specks and discontinuous laminae of FeS. One nodule 3 mm across of glauconite at 18 cm Section 2. In Sections 2 and 3 pale yellowish brown (10YR 6/2) intervals alternate with olive gray (5Y 6/1) to light gray (N7) CLAYEY GLAUCONITIC NANNOFOSSIL OOZE layers.																														
	CG			1.0																																		
middle Miocene	N12–14 (F) NN7–10 (N)				2		* *	AR: Acid residue, fraction >30µ: Quartz 65 Glauconite 25 Framboidal pyrite 5 Heavy minerals 1 White mica 3 SMEAR SLIDE SUMMARY (%): <table><tr><td></td><td>1, 78</td><td>2, 18</td><td>2, 107</td><td>3, 137</td></tr><tr><td></td><td>D</td><td>M</td><td>D</td><td>D</td></tr><tr><td>Texture:</td><td></td><td></td><td></td><td></td></tr><tr><td>Sand</td><td>1</td><td>30</td><td>1</td><td>3</td></tr><tr><td>Silt</td><td>1</td><td>10</td><td>4</td><td>2</td></tr><tr><td>Clay</td><td>96</td><td>60</td><td>95</td><td>95</td></tr></table> Composition: Quartz Tr Tr Tr Tr Heavy minerals – Tr – – Clay 5 5 5 5 Glauconite – 30 – – Pyrite – Tr Tr Tr Tr Foraminifers Tr Tr Tr 3 Calc. nannofossils 95 60 90 90 Pteropods – Tr – – Dolomite Tr Tr Tr Tr		1, 78	2, 18	2, 107	3, 137		D	M	D	D	Texture:					Sand	1	30	1	3	Silt	1	10	4	2	Clay	96	60	95	95
		1, 78	2, 18	2, 107	3, 137																																	
	D	M	D	D																																		
Texture:																																						
Sand	1	30	1	3																																		
Silt	1	10	4	2																																		
Clay	96	60	95	95																																		
	N12–14 (F) NN7–10 (N)	AG			3		* *	ORGANIC CARBON AND CARBONATE (%): <table><tr><td></td><td>1, 130–132</td><td>2, 10–12</td></tr><tr><td>Carbonate</td><td>61.0</td><td>67.3</td></tr></table>		1, 130–132	2, 10–12	Carbonate	61.0	67.3																								
	1, 130–132	2, 10–12																																				
Carbonate	61.0	67.3																																				
	AG	RP	B	CC																																		

SITE 544 HOLE A CORE 8 CORED INTERVAL 64.0–73.5 m sub-bottom

TIME – ROCK UNIT	BIOSTRATIGRAPHIC ZONE	FOSSIL CHARACTER			SECTION METERS	GRAPHIC LITHOLOGY	DRILLING RECORD DISTANCE SAMPLING STRUCTURES	LITHOLOGIC DESCRIPTION																																													
		FORAMINIFERS	NANNOFOSSILS	RADIOLARIANS					DIATOMS																																												
middle Miocene	N14–12 (F)				0.5		* *	Slightly disturbed pale yellowish brown (10YR 6/2) and light olive gray (5Y 6/1) CLAYEY FORAMINIFERAL NANNOFOSSIL OOZE and NANNOFOSSIL OOZE. Alternating zones of 30–40 cm thickness of lighter gray and slightly darker brownish sediment. Indistinct laminations and layers of 3 mm to 4 cm thickness. Some medium light gray to medium dark gray FeS rich layers and specks in Section 3. Dark green GLAUCONITIC layer at Section 3, 105 cm.																																													
				1.0																																																	
				2																																																	
				3																																																	
	N14–12 (F)				4		* *	SMEAR SLIDE SUMMARY (%): <table><tr><td>Texture:</td><td>4, 50</td><td>D</td></tr><tr><td>Sand</td><td>10</td><td></td></tr><tr><td>Silt</td><td>20</td><td></td></tr><tr><td>Clay</td><td>70</td><td></td></tr><tr><td>Composition:</td><td></td><td></td></tr><tr><td>Quartz</td><td>5</td><td></td></tr><tr><td>Feldspar</td><td>Tr</td><td></td></tr><tr><td>Mica</td><td>Tr</td><td></td></tr><tr><td>Heavy minerals</td><td>Tr</td><td></td></tr><tr><td>Clay</td><td>10</td><td></td></tr><tr><td>Glauconite</td><td>Tr</td><td></td></tr><tr><td>Pyrite</td><td>Tr</td><td></td></tr><tr><td>Foraminifers</td><td>10</td><td></td></tr><tr><td>Calc. nannofossils</td><td>70</td><td></td></tr><tr><td>Dolomite</td><td>Tr</td><td></td></tr></table>	Texture:	4, 50	D	Sand	10		Silt	20		Clay	70		Composition:			Quartz	5		Feldspar	Tr		Mica	Tr		Heavy minerals	Tr		Clay	10		Glauconite	Tr		Pyrite	Tr		Foraminifers	10		Calc. nannofossils	70		Dolomite	Tr	
Texture:	4, 50	D																																																			
Sand	10																																																				
Silt	20																																																				
Clay	70																																																				
Composition:																																																					
Quartz	5																																																				
Feldspar	Tr																																																				
Mica	Tr																																																				
Heavy minerals	Tr																																																				
Clay	10																																																				
Glauconite	Tr																																																				
Pyrite	Tr																																																				
Foraminifers	10																																																				
Calc. nannofossils	70																																																				
Dolomite	Tr																																																				
				CC				ORGANIC CARBON AND CARBONATE (%): <table><tr><td>Carbonate</td><td>2, 20–22</td><td>2, 144–150</td></tr><tr><td></td><td>79.9</td><td>77.1</td></tr><tr><td></td><td>3, 118–120</td><td>4, 0–2</td></tr><tr><td>Carbonate</td><td>76.1</td><td>71.6</td></tr></table>	Carbonate	2, 20–22	2, 144–150		79.9	77.1		3, 118–120	4, 0–2	Carbonate	76.1	71.6																																	
Carbonate	2, 20–22	2, 144–150																																																			
	79.9	77.1																																																			
	3, 118–120	4, 0–2																																																			
Carbonate	76.1	71.6																																																			
		AG	FM																																																		

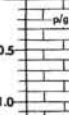

SITE 544 HOLE A CORE 11 CORED INTERVAL 92.5–102.0 m sub-bottom									
TIME – ROCK UNIT	BIOSTRATIGRAPHIC ZONE	FOSSIL CHARACTER				SECTION	METERS	GRAPHIC LITHOLOGY	LITHOLOGIC DESCRIPTION
		FORAMINIFERS	NANNOFOSSILS	RADIOLARIANS	DIATOMS				
early middle Miocene	N9–11 (F)	AG	CG			1	0.5		Highly disturbed, pinkish gray (5YR 8/1) to grayish orange pink (5YR 7/2) CLAYEY FORAMINIFERAL NANNOFOSSIL OOZE with some Fe/Mn mottles and burrow fills.
	<i>Shenolthus heteromorphus</i> zone (NNS) (N)								SMEAR SLIDE SUMMARY (%): 1, 30 D Composition: Quartz Tr Clay 20 Foraminifers 20 Calc. nannofossils 60 Dolomite Tr


SITE 544 HOLE A CORE 12 CORED INTERVAL 102.0–107.5 m sub-bottom									
TIME – ROCK UNIT	BIOSTRATIGRAPHIC ZONE	FOSSIL CHARACTER				SECTION	METERS	GRAPHIC LITHOLOGY	LITHOLOGIC DESCRIPTION
		FORAMINIFERS	NANNOFOSSILS	RADIOLARIANS	DIATOMS				
early middle Miocene	N9 (F)	AG	CG			1	0.5		Section 1, 0–60 cm: slightly disturbed, light greenish gray (5GY 8/1) VERY CLAYEY FORAMINIFERAL NANNOFOSSIL OOZE mottled, firm, grains of glauconite.
early Miocene	N7 (F) NNS (N)	AG				1	1.0		Section 1, 60–74 cm: sharply bounded, slightly disturbed, dusky green (5G 3/2) and mottled dusky red (5G 3/2) GLAUCONITIC CLAYEY FORAMINIFERAL NANNOFOSSIL OOZE to LIMESTONE, topped and bottomed by cm thick horizons of greenish black (5GY 2/1) GLAUCONITE.
early Miocene	<i>Globigerinella insuata</i> zone (N7) (F) NNS (N)	FM	RP			2			Section 1, 74–95 cm: slightly disturbed, yellowish gray (5Y 8/1) VERY CLAYEY CALCAREOUS OOZE, traces of mottling.
Middle to Late Jurassic	N3–5 (N)					CC			Section 1, 95–148 cm; Section 2, 0–18 cm; and Core-Catcher, 0–6 cm: slightly disturbed, grayish yellow-green (5GY 7/2) NANNOFOSSIL-BEARING CLAY with mm to cm sized limonitic patches and nodules.
									Core-Catcher, 6–12 cm: SKELETAL-PELOID PACKSTONE as in Core 13.
									SMEAR SLIDE SUMMARY (%): 1, 4 1, 56 1, 62 1, 72 1, 80 2, 6 D D D D D D Texture: Sand 10 5 15 10 – – Silt 15 10 25 30 5 – Clay 75 85 60 60 85 – Composition: Quartz – – 10 10 2 – Clay 12 8 15 30 – – Glauconite – – 10 30 1 – Limonite – – – – 100 Fe-oxides – – 5 – – – Carbonate unsp./micrite – – – 5 93 – Foraminifers 18 15 15 – – – Calc. nannofossils 70 77 45 20 2 – Dolomite 1 – – 5 2 – 2, 10 2, 18 CC D D D Texture: Sand – – Tr Silt 1 1 25 Clay 99 99 75 Composition: Quartz – – 10 Mica Tr Tr – Clay 90 90 60 Calc. nannofossils 7 7 15 Sponge spicules Tr – – Dolomite 1 2 15
									THIN SECTION/PEEL SUMMARY (%): CC, 12 Texture: Rudite 10 Arenite 70 Silt 20 Composition: Micrite 95 Sparite 5 Intraclasts 10 Oncoids } Coated grains } Ooids } Peloids } Bioclasts } Skeletal grains: Crinoids Tr Bivalves Tr Gastropods Tr Forams Tr Sol. corals Tr Echin. spines Tr Ostracods Tr
									ORGANIC CARBON AND CARBONATE (%): 1, 37–39 1, 39–40 2, 11–13 Carbonate 58.5 74.1 3.1

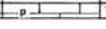
SITE 544 HOLE A CORE 13 CORED INTERVAL 107.5–111.5 m sub-bottom									
TIME – ROCK UNIT	BIOSTRATIGRAPHIC ZONE	FOSSIL CHARACTER				SECTION	METERS	GRAPHIC LITHOLOGY	LITHOLOGIC DESCRIPTION
		FORAMINIFERS	NANNOFOSSILS	RADIOLARIANS	DIATOMS				
Middle to Late Jurassic	<i>Protoglobigerina</i> sp. <i>Globobulimina alba</i>					1	0.5		Highly fractured (2–18 cm pieces), pale reddish brown (10R 5/4), grayish orange (10YR 7/4) and pale yellowish brown (10YR 6/2) SKELETAL INTRACLAST-PELOID PACKSTONE with patches of GRAINSTONE. Several "HARDGROUNDS": sharp boundaries cutting through grains, with irregular limonite coatings. Abundant subhorizontal vugs with horizontal geopetal infill of fine calcarenitic (diagenetic) sediment and sparry cement (rare open drusy cavities). Skeletal grains include numerous ammonites, "pelagic" bivalves (filaments), crinoids, gastropods, ostracods, etc., many with micritic or limonitic coatings. Common oncoids. Color mottling.
						2	1.0		THIN SECTION/PEEL SUMMARY (%): 1, 22–27 1, 75–82 2, 39–44 2, 53–56 Texture: Rudite 20 20 15 5 Arenite 60 40 75 95 Silt 20 40 10 – Composition: Micrite 90 100 50 10 Sparite 10 – 50 90 Intraclasts 20 Tr 10 Tr Oncoids } Coated grains } Ooids } Peloids } Bioclasts } Skeletal grains: Crinoids Tr Tr Tr Tr Bivalves Tr Tr Tr Tr Gastropods Tr Tr Tr Tr Ammonites Tr – Tr – Brachiopods Tr – – – Serpulids Tr Tr – Tr Forams Tr Tr – Tr Ostracods Tr – – – Sponge spic. Tr – – – Quartz Tr – – – Structure: Geopetal fab. Tr Tr – Hardground Tr – Tr Tr

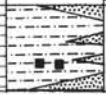
SITE 544		HOLE A		CORE 14	CORED INTERVAL		111.5–121.0 m sub-bottom	
TIME – ROCK UNIT	BIOSTRATIGRAPHIC ZONE	FOSSIL CHARACTER			SECTION METERS	GRAPHIC LITHOLOGY	DRILLING DISTURBANCE STRUCTURES	SAMPLES
		FORAMINIFERS	NANNOFOSILS	RADIOLARIANS				
Middle to Late Jurassic	<i>Protoglobigerina</i> sp. <i>Gracilohoplites</i> sp.				1	p/g		
					1.0			
					2	p/g		
					3	p/g		
					4			
<p>Highly fractured (2–18 cm pieces), pale reddish brown (10R 5/4), yellowish gray (5Y 7/2) and pale yellowish brown (10YR 6/2) PELOID INTRACLAST SKELETAL PACK- TO GRAINSTONE similar to Core 13.</p> <p>Frequent subhorizontal calcite filled vugs throughout, Section 4, 86–125 cm shows fine irregular mottling, limonite filling voids and staining micrite. Skeletal grains include abundant crinoid stem fragments (mostly <i>Pentacrinites</i>) up to 2 cm length, particularly abundant in certain levels (Section 1, 22–47 cm; Section 4, 15–23, 55–85, and 108–113 cm). Generally poorly sorted, bioturbated. Rare sponge fragments (Section 4, 20 cm).</p> <p>THIN SECTION/PEEL SUMMARY (%): 4, 100</p> <p>Composition: Micrite 30 Peloids 30 Skeletal grains: Crinoids 30 Bivalves 5 Forams 3 Limonite Tr</p>								

SITE 544		HOLE A		CORE 15	CORED INTERVAL		121.0–130.0 m sub-bottom	
TIME – ROCK UNIT	BIOSTRATIGRAPHIC ZONE	FOSSIL CHARACTER			SECTION METERS	GRAPHIC LITHOLOGY	DRILLING DISTURBANCE STRUCTURES	SAMPLES
		FORAMINIFERS	NANNOFOSILS	RADIOLARIANS				
Jurassic	<i>Protoglobigerina</i> <i>nodosulcata, milloids, spirulina, lentitulina, itaculida, ammoniaculites</i>				1	p/g		
					1.0			
					2	p		
					3	p		
					4			
<p>Section 1, 0–20, 72–150 cm and Section 2 through 4: INTRACLAST PELOID ONKOIDAL SKELETAL PACK- AND GRAINSTONE as described in Cores 13 and 14.</p> <p>Section 1, 20–72 cm: grayish orange-pink (5YR 7/2), yellowish gray (5Y 7/2) and pale olive (10Y 6/2) INTRACLAST SKELETAL PACK- STONE. Intraclasts angular to rounded up to 3 cm across in skeletal-peloidal slightly clayey matrix. Geopetally filled voids common, 1 cm thick psilotic to oolitic layers, few argillaceous laminae (25–31 cm). At 28 cm a fragment of <i>7dasyclad</i> algae.</p> <p>Section 2, 94 cm: entire echinid body.</p> <p>Section 3, 70 cm: dissolution surface cutting through grains, cut by vertical calcite vein which shortly follows hardground and is anastomosing with sparry cement in grainstone above.</p> <p>THIN SECTION/PEEL SUMMARY (%): 3, 70–73</p> <p>Texture: Rudite 10 Arenite 50 Silt 40</p> <p>Composition: Micrite 70 Sparite 30 Intraclasts Tr Oncolids Coated grains } 80 Ooids Peloids Bioclasts 20 Skeletal grains: Crinoids Tr Bivalves Tr Gastropods Tr Forams Tr Ostracods Tr</p> <p>Structure: Hardground Tr</p> <p>ORGANIC CARBON AND CARBONATE (%): 3, 102–104 Carbonate bomb 100</p>								

SITE 544		HOLE A		CORE 16		CORED INTERVAL		130.0–139.0 m sub-bottom	
TIME – ROCK UNIT	BIOSTRATIGRAPHIC ZONE	FOSSIL CHARACTER			SECTION METERS	GRAPHIC LITHOLOGY	DRILLING DISTURBANCE STRUCTURES	SAMPLES	LITHOLOGIC DESCRIPTION
		FORAMINIFERS	NANNOFOSILS	RADIOLARIANS					
Jurassic					1				<p>Highly fractured, pale yellowish orange (10YR 8/6) and pale reddish brown (10R 5/4) to dark yellowish orange (10YR 6/6) INTRACLASTIC ONCOLITH SKELETAL PACKSTONE to GRAINSTONE as described in Cores 13 through 15.</p> <p>Shallow water derived particles get more abundant: <i>milolids</i>, foraminiferal oncolids, "pelagic" bivalves and ammonites rare at base of core. Geopetally filled, flat floored vugs common throughout as in Cores 13 through 15 (rare partially open voids).</p>
				0.5					
						1.0			


SITE	544	HOLE A	CORE 17	CORED INTERVAL	139.0–148.0 m sub-bottom
TIME – ROCK UNIT	BIOSTRATIGRAPHIC ZONE	FOSSIL CHARACTER	SECTION METERS	GRAPHIC LITHOLOGY	LITHOLOGIC DESCRIPTION
		FORAMINIFERS NANNOFOSILS RADIOLARIANS DIATOMS			
		B B B	1		<p>Section 1, 0–22 cm: highly fractured, moderate reddish orange (10R 6/6) SKELETAL PELOID INTRACLAST PACKSTONE with patches of GRAINSTONE as described in Cores 13 through 16. Superficial ooids, oncoids, and geopetally filled voids are common. Contact not preserved.</p> <p>Section 1, 22–27 cm: highly disturbed, dark reddish brown (10R 3/4) SANDY CLAY 5–15% coarse grained limonite-stained quartz, rare silt- to fine sand-sized dolomite rhombs.</p> <p>SMEAR SLIDE SUMMARY (%):</p> <p>1, 26 D</p> <p>Texture:</p> <p>Sand (all removed) – Silt 25 Clay 75</p> <p>Composition:</p> <p>Quartz 20 Feldspar 3 Heavy minerals 1 Clay 75 Dolomite 1</p> <p>THIN SECTION/PEEL SUMMARY (%):</p> <p>1, 14–16</p> <p>Texture:</p> <p>Rudite 15 Arenite 80 Silt 5</p> <p>Composition:</p> <p>Micrite 10 Sparite 90 Intraclasts Tr Oncoids } Coated grains } 80 Ooids } Bioclasts 20 Skeletal grains: Crinoids Tr Bivalves Tr Gastropods Tr Brachiopods Tr Serpulids Tr Forams Tr Echinoid spin. Tr Ostracods Tr Bryozoans Tr</p> <p>Structure:</p> <p>Vugs Tr</p> <p>ORGANIC CARBON AND CARBONATE (%):</p> <p>1, 26–37 Carboante bomb 11.5</p>

SITE	544	HOLE A	CORE 18	CORED INTERVAL	148.0–149.5 m sub-bottom
TIME – ROCK UNIT	BIOSTRATIGRAPHIC ZONE	FOSSIL CHARACTER	SECTION METERS	GRAPHIC LITHOLOGY	LITHOLOGIC DESCRIPTION
		FORAMINIFERS NANNOFOSILS RADIOLARIANS DIATOMS			
			1		<p>Highly fractured, moderate orange pink (10R 7/4) SKELETAL PELOID INTRACLAST PACKSTONE as described in Cores 13 through 17. Reddish SANDY CLAY sits on surface of topmost limestone fragment.</p>

SITE	544	HOLE A	CORE 19	CORED INTERVAL	149.5–157.0 m sub-bottom
TIME – ROCK UNIT	BIOSTRATIGRAPHIC ZONE	FOSSIL CHARACTER	SECTION METERS	GRAPHIC LITHOLOGY	LITHOLOGIC DESCRIPTION
		FORAMINIFERS NANNOFOSILS RADIOLARIANS DIATOMS			
		B B B B	1 0.5		<p>Slightly to highly disturbed, 93% dark reddish brown (10R 3/4) and 7% pale olive (10Y 6/2) CALCAREOUS SANDY MUD to MUDDY SAND with finer color interlayering. Quartz ranges from fine to medium sand-size (mean) to granule size. Calcareous sand concentrations at 0–3, 13–30, 35–41, 50–53, 63–65, and 75–81 cm.</p> <p>In Section 1, 52–68 cm, slightly disturbed pale olive (10Y 6/2) wisps alternate with red colored lithology. At 55–56 and 58–60 cm two pale orange (10R 8/2) rounded MICRITIC LIMESTONE concretions.</p> <p>ORGANIC CARBON AND CARBONATE (%):</p> <p>1, 79–81 Carbonate 3.7</p>

SITE 544		HOLE A		CORE 20		CORED INTERVAL		157.0-166.0 m sub-bottom								
TIME - ROCK UNIT	BIOSTRATIGRAPHIC ZONE	FOSSIL CHARACTER				SECTION	METERS	GRAPHIC LITHOLOGY	DRILLING DISTURBANCE EXTRINSIC SEDIMENTARY STRUCTURES	SAMPLES	LITHOLOGIC DESCRIPTION					
		FORAMINIFERA	NANNOFOSSILS	RADIOLARIANS	DIAFORES											
Triassic to Hettangian? with downworked Jurassic limestone	B					1	0.5 1.0				<p>Section 1, 0-132 cm; Section 2, 0-120 cm; and Section 3, 42-160 cm: slightly disturbed, grayish red (10R 4/2) CALCAREOUS SANDY MUD with laminae of MUDDY SAND with minor blebs and wisps of gray olive (10Y 4/2) less SANDY CLAY. Sand constitutes 30-60% of rock: very fine sand to granule sized grains of quartz (76%), feldspar (15%), micritic carbonate clasts (10%) and minor amounts of mica, illinite(?), sphere(?). Several MUDSTONE clasts at Section 3, 82-112 cm.</p>					
						2					<p>Section 1, 132-160 cm; Section 3, 0-42 cm; and Section 4, 0-15 cm: slightly disturbed, color mottled, grayish red (10R 4/2) and light olive gray (5Y 5/2) to gray olive (10Y 4/2) CALCAREOUS SANDY MUD and MUDDY SAND. Gray mottles often contain more sand and/or more dolomite and calcite.</p>					
											<p>BIOCLASTIC LIMESTONE clast at Section 1, 5-8 cm.</p>					
											<p>ORGANIC CARBON AND CARBONATE (%):</p> <table border="1"> <tr> <td>2, 118-126</td> <td>3, 0-2</td> <td>3, 5-6</td> </tr> <tr> <td>Carbonate</td> <td>18.3</td> <td>14.1</td> <td>16.7</td> </tr> </table>	2, 118-126	3, 0-2	3, 5-6	Carbonate	18.3
2, 118-126	3, 0-2	3, 5-6														
Carbonate	18.3	14.1	16.7													

SITE	544	HOLE	A	CORE	21	CORED INTERVAL						166.0–175.0 m sub-bottom
TIME – ROCK UNIT	BIOSTRATIGRAPHIC ZONE	FOSSIL CHARACTER				SECTION	METERS	GRAPHIC LITHOLOGY	DISTURBED SECONDARY STRUCTURES	SAMPLES	LITHOLOGIC DESCRIPTION	
		FORAMINIFERS	NANNOPHYCIDS	RADIOLARIANS	DIATOMS							
Triassic to Hettangian?											Section 1, 10–100 cm: slightly disturbed, color mottled, grayish red (10R 4/2) and light olive gray (5Y 5/2) CALCAREOUS SANDY MUD with laminae and layers of MUDDY SAND. Lithology similar to Core 20, generally less sand. Some soft sediment deformation at Section 1, 20–30 cm.	
											Section 1, 100–146 cm and Section 2, 0–84 cm: slightly to moderately fractured, reddish brown (10R 4/4) MUDSTONE with minor amounts of dispersed sand and some sandy layers abundant microfractures occur throughout. They show light olive gray (5Y 2) reduction halos. Evident soft sediment deformation. Some horizontal pink (5YR 8/4) calcite laminae (calcite stringers?) in Section 2.	

SITE	544	HOLE	A	CORE	22	CORED INTERVAL	175.0-184.5 m sub-bottom
TIME - ROCK UNIT	BIOSTRATIGRAPHIC ZONE	FOSSIL CHARACTER		SECTION	METERS	GRAPHIC LITHOLOGY	LITHOLOGIC DESCRIPTION
	FORAMINIFERS	NAUWFOSSILS	RADICULARIANS			ROLLING DISTURBANCE	
		DINOTRANS				SEDIMENTARY STRUCTURES	
						SAMPLES	
7Rhaician to Hetangian?				1	0.5		<p>Section 1, 0-57 cm: slightly fractured, reddish brown (10R 4/4) SANDY MUDESTONE with light olive gray (SY 5/2) microfractures throughout as Core 21.</p> <p>Section 1, 57-83 cm: highly fractured grayish red (10R 4/2) PEBBLY COARSE SANDY angular grains and pebbles up to 2 cm across of weathered gneiss and feldspar, quartz poorly sorted, grain supported, clayey matrix.</p> <p>Section 1, 83-96 cm: three pebbles of granite-gneiss, two with weathered surfaces, one cut by coring, and one fresh granite-gneiss cobble.</p>
<p>THIN SECTION/PEEL SUMMARY (%): 1, 88-92</p> <p>Composition:</p> <ul style="list-style-type: none"> Plagioclase 30 Biotite 2 Quartz 30 Alkali feldspar 30 Microcline 30 Muscovite 0.5 							

SITE 544		HOLE A		CORE 23		CORED INTERVAL		184.0–193.0 m sub-bottom	
TIME – ROCK UNIT	BIOSTRATIGRAPHIC ZONE	FOSSIL CHARACTER				SECTION	METERS	GRAPHIC LITHOLOGY	LITHOLOGIC DESCRIPTION
		FORAMINIFERA	NAUPODIDAE	RADIOLARIANS	DICATONS				
?	B	B	B	B	B	1			<p>Highly fractured to brecciated, reddish brown (10R 4/4) and pale red (10R 6/2) GRANITE-GNEISS BRECCIA. Two pebbles (topmost and at approximately 23 cm – drilling breccia) similar to cobble at base of Core 22. Two other 4–6 cm pebbles and several smaller of highly weathered strongly foliated gneiss. Highly weathered clayey arcotic sand, "matrix" mostly washed out by drilling.</p>

SITE 544		HOLE A		CORE 24		CORED INTERVAL		193.0–202.0 m sub-bottom		
TIME – ROCK UNIT	BIOSTRATIGRAPHIC ZONE	FOSSIL CHARACTER				SECTION	METERS	GRAPHIC LITHOLOGY	DRILLING DISTURBANCE STRUCTURE STRUCTURE SAMPLES	LITHOLOGIC DESCRIPTION
		FORAMINIFERS	NAUPODOLITES	RADIOLARIANS	Diatoms					
Cambrian basement						1				<p>Fourteen pieces 4–5 cm across and 3 pieces 2–3 cm across of grayish red (5R 4/2 to 10R 4/2) GRANITE GNEISS.</p> <p>Foliated on a 2–3 mm scale. Feldspars 5 mm–1 cm sized have porphyroblastic shapes.</p> <p>Fracture joints at approximately right angle to foliation.</p>
						0.5				

SITE 544		HOLE B		CORE 10		CORED INTERVAL		33.7–36.4 m sub-bottom	
TIME – ROCK UNIT	BIOSTRATIGRAPHIC ZONE	FOSSIL CHARACTER			SECTION METERS	GRAPHIC LITHOLOGY	DRILLING DISTURBANCE SEDIMENTARY STRUCTURES SAMPLES	LITHOLOGIC DESCRIPTION	
		FORAMINIFERS	NANNOFOSSILS	RADIOLARIANS					
Late Miocene to early Pliocene	N17–18 (F) NN17 (N)	CG			1			Below soupy top mostly undisturbed, grayish orange pink (5YR 7/2) to pale yellowish brown (10YR 6/2) CLAYEY NANNOFOSSIL OOZE with undistinct laminae and minor horizontal blackish specks throughout.	
					2				

SITE 544		HOLE B		CORE 11		CORED INTERVAL		36.4–37.4 m sub-bottom	
TIME – ROCK UNIT	BIOSTRATIGRAPHIC ZONE	FOSSIL CHARACTER			SECTION METERS	GRAPHIC LITHOLOGY	DRILLING DISTURBANCE SEDIMENTARY STRUCTURES SAMPLES	LITHOLOGIC DESCRIPTION	
		FORAMINIFERS	NANNOFOSSILS	RADIOLARIANS					
Late Miocene	N17 (F) upper half of NN11 (N)	CG			1			Mostly undisturbed rather stiff, grayish orange pink (5YR 7/2) to pale yellowish brown (10YR 6/2) CLAYEY NANNOFOSSIL OOZE as in Core 10.	
					2				

SITE 544		HOLE B		CORE 12		CORED INTERVAL		37.4–39.3 m sub-bottom	
TIME – ROCK UNIT	BIOSTRATIGRAPHIC ZONE	FOSSIL CHARACTER			SECTION METERS	GRAPHIC LITHOLOGY	DRILLING DISTURBANCE SEDIMENTARY STRUCTURES SAMPLES	LITHOLOGIC DESCRIPTION	
		FORAMINIFERS	NANNOFOSSILS	RADIOLARIANS					
Late Miocene	N17 (F) upper half of NN11 (N)	B			1			Partly soupy, partly slightly disturbed grayish orange pink (5YR 7/2) to pale yellowish brown (10YR 6/2) CLAYEY NANNOFOSSIL OOZE as in Cores 10 and 11.	
					2				

